

School of Energy and Power Engineering
 Direction 13.04.02 Electric power industry and electrical engineering
 Department for Power and Electrical Engineering

MASTER'S THESIS

Topic of work
Разработка алгоритма управления сетевым инвертором генерирующих установок на базе возобновляемых источников энергии/ The algorithm for controlling the network inverter of generating plants based on renewable energy sources development

УДК 621.314.572:620.92

To student:

Group	Full name	Signature	Date
5AM1Ch	Boris Dmitrievich Maliuta		

Head of FQW:

Position	Full name	Academic degree, title	Signature	Date
Associate Professor of TPU	Alexei Alexandrovich Suvorov	Candidate of Technical Sciences		

CONSULTANTS FOR SECTIONS:

In the section «Financial management, resource efficiency and resource saving»

Position	Full name	Academic degree, title	Signature	Date
Associate Professor of TPU	Lyubov Yurievna Spitsyna	Candidate of Economic Sciences		

In the section «Social responsibility»

Position	Full name	Academic degree, title	Signature	Date
Associate Professor of TPU	Olga Alekseevna Antonevich	Candidate of Biological Sciences		

In the section «Foreign Languages»

Position	Full name	Academic degree title	Signature	Date
Senior Lecturer	Olga Mikhailovna Demidova	-		
Associate Professor of TPU	Irina Anatolyevna Chesnokova	Candidate of Philological sciences		

ADMIT TO DEFENSE:

Position	Full name	Academic degree, title	Signature	Date
Associate Professor of TPU	Mikhail Alexandrovich Surkov	Candidate of Technical Sciences		

Planned learning outcomes for the MEP

Result code	Learning Outcome
<i>Universal competencies</i>	
P1	To improve and develop one's intellectual and general cultural level, to achieve moral and physical improvement of one's personality, to teach new methods of research, to change the scientific and scientific-production profile of one's professional activity.
P2	Freely use Russian and foreign languages as a means of business communication, the ability for active social mobility
P3	Use in practice the skills and abilities in the organization of research and production work, in team management, use knowledge of legal and ethical standards in assessing the consequences of their professional activities.
P4	To have an idea about the methodological foundations of scientific knowledge and creativity, the role of scientific information in the development of the industry, the skills of working with the involvement of modern information technologies, to synthesize and critically summarize information.
<i>Professional competencies</i>	
P5	Apply in-depth scientific, mathematical, socio-economic and professional knowledge in an interdisciplinary context in innovative engineering activities in the field of electric power and electrical engineering.
P6	Set and solve innovative problems of engineering analysis in the field of electric power industry and electrical engineering using deep fundamental and special knowledge, analytical methods and complex models under uncertainty.
P7	Carry out engineering projects using original design methods to achieve new results that provide competitive advantages for electric power and electrical production in the face of severe economic and environmental constraints.
P8	Conduct innovative engineering research in the field of electric power and electrical engineering, including a critical analysis of data from the world's information resources.
P9	Conduct a feasibility study of design solutions; perform organizational and planning calculations for the creation or reorganization of production sites, plan the work of personnel and payroll funds; determine and provide effective modes of the technological process.
P10	Carry out installation, adjustment, testing, adjustment work of electric power and electrical equipment.
P11	To master new electric power and electrical equipment; check the technical condition and residual life of the equipment and organize routine inspection and maintenance.
P12	Develop working design and scientific and technical documentation in accordance with standards, specifications and other regulatory documents; organize metrological support of electric power and electrical equipment; draw up operational documentation provided for by the rules for the technical operation of equipment and the organization of work.

School of Energy and Power Engineering
 Direction 13.04.02 Electric power industry and electrical engineering
 Department of Electricity and Electrical Engineering

APPROVE:
 Head of the MEP
 Mikhail A. Surkov
 «__» _____

EXERCISE
for the completion of the final qualifying work

In the form of:

Master's Thesis

To student:

Group	Full name
5AM1Ch	Boris Dmitrievich Maliuta

Topic of work:

Разработка алгоритма управления сетевым инвертором генерирующих установок на базе возобновляемых источников энергии/ The algorithm for controlling the network inverter of generating plants based on renewable energy sources development		
<table border="1" style="width: 100%;"> <tr> <td style="width: 60%;">Approved by the director's order (date, number)</td> <td style="text-align: center;">09.02.2023 40-12/c</td> </tr> </table>	Approved by the director's order (date, number)	09.02.2023 40-12/c
Approved by the director's order (date, number)	09.02.2023 40-12/c	

Deadline for student submission of completed work:	07.06.2023
----------------------------------------------------	------------

TECHNICAL TASK:

Initial data for work	– Current-controlled virtual synchronous generator topology
List of research, design and development issues	In the RW was considered the problem of integration of renewable energy sources in power systems. Different approaches of its solving were investigated and topology of current-controlled VSG was proposed and investigated. Related studies are "Financial Management, Resource Efficiency and Resource Saving" in which the effectiveness of STI was evaluated and "Social Responsibility", in which issues of ensuring life safety were considered.
List of graphic material <i>(with exact specification of required drawings)</i>	There is no graphic material
Consultants for the sections of the final qualifying work <i>(with sections indicated)</i>	
Section	Consultant
Social responsibility	Candidate of Biological Sciences, Associate Professor Antonevich Olga Alekseevna

Financial management	Candidate of Economics, Associate Professor Lyubov Yurievna Spitsyna
Foreign language	Senior Lecturer Olga Mikhailovna Demidova
	Candidate of Philological Sciences, Associate Professor Irina Anatolyevna Chesnokova
Titles of sections that must be written in a foreign language:	
Introduction; Green Energy. Current positions, trends and problems; Virtual synchronous generator; Investigation of VSG-C topology; Financial management, resource efficiency and resource saving; Social responsibility; Conclusion;	

Date of issue of the assignment for the completion of the final qualification work according to the linear schedule	29.01.2023
----------------------------------------------------------------------------------------------------------------------------	------------

The task was given by the head of FQW:

Position	Full name	Academic degree, title	Signature	Date
Associate Professor of TPU	Alexei Alexandrovich Suvorov	Candidate of Technical Sciences		01.02.2023

The task was accepted by the student:

Group	Full name	Signature	Date
5AM1Ch	Boris Dmitrievich Maliuta		01.02.2023

School of Energy and Power Engineering

Direction 13.04.02 Electric power industry and electrical engineering

Department of Electricity and Electrical Engineering

CALENDAR PLAN
completion of the final qualifying work

Deadline for student submission of completed work:	07.06.2023
----------------------------------------------------	------------

Control date	Title of section (module) / type of work (research)	Maximum section (module) score
05.03.22	Literature review	10
02.04.22	Introduction	5
23.04.23	Task calculations	10
21.05.23	Research results	5
22.05.23	Financial management, resource efficiency and resource saving.	5
25.05.23	Social responsibility	5
		40

Compiled by the head of FQW:

Position	Full name	Academic degree, title	Signature	Date
Associate Professor of TPU	Alexei Alexandrovich Suvorov	Candidate of Technical Sci- ences		15.01.2023

AGREED:

Head of the MEP	Full name	Academic degree, title	Signature	Date
13.04.02 Electric power industry and electrical engineer- ing	Mikhail Alexandro- vich Surkov	Candidate of Technical Sci- ences		

**TASK FOR SECTION
«FINANCIAL MANAGEMENT, RESOURCE EFFICIENCY AND RESOURCE SAVING»**

Group name	Full name
5AM1Ch	Boris Dmitrievich Maliuta

School	School of Energy and Power Engineering	Department	Division for Power and Electrical Engineering
Education	Master's degree	Specialty	13.04.02 Electric Power and Electrical Engineering

Initial data for the section «Financial management, resource efficiency and resource saving»:	
1. The cost of research resources: logistical, energy, financial, information and human resources	The project budget is no more than 500 000 rubles, including labour costs of no more than 280 000 rubles.
2. Norms and standards for the use of resources	Integral resource efficiency score of at least 4.3 out of 5
3. The taxation system used, tax rates, deductions, discounting and crediting	Contributions to extra-budgetary funds are 30%
A list of issues to be researched, designed and developed:	
1. Assessing the commercial and innovation potential of STI	Analysis and assessment of the scientific and technical level of the project (STI)
2. Drafting the statutes of a science and technology project	Not being developed
3. Planning the STI management process: structure and schedule, budget, risks and procurement	Development of a timetable and cost estimate.
4. Determination resource, financial, economic efficiency	Determining resource efficiency
List of graphic material (with exact indication of the required drawings):	
1. Assessing the competitiveness of technical solutions 2. FAST diagram 3. SWOT matrix 4. STI timetable and budget 5. Assessing the resource, financial and economic efficiency of STI	

Date of issue of the task for the section according to the linear schedule	01.03.2023
-----------------------------------------------------------------------------------	-------------------

The task was given by the consultant:

Position	Full name	Academic degree	Signature	Date
Associate Professor of TPU	Spitsyna Lyubov Yurievna	Candidate of Economical Sciences		

The task was accepted by the student:

Group	Full name	Signature	Date
5AM1Ch	Boris Dmitrievich Maliuta		01.03.2023

Разработка алгоритма управления сетевым инвертором генерирующих установок на базе возобновляемых источников энергии/ The algorithm for controlling the network inverter of generating plants based on renewable energy sources development

To student:

Group	Full name	Date	Date
5AM1Ch	Boris Dmitrievich Maliuta		

Head of FQW:

Position	Full name	Academic degree title	Signature	Date
Associate Professor of TPU	Alexei Alexandrovich Suvorov	Candidate of Technical Sciences		

Consultant - linguist of the Department of Foreign Languages:

Position	Full name	Academic degree title	Signature	Date
Senior Lecturer	Olga Mikhailovna Demidova	-		
Associate Professor of TPU	Irina Anatolyevna Chesnokova	Candidate of Philological sciences		

Contents

Abstract.....	11
Introduction.....	12
1. Green Energy. Current position, trends and problems.....	14
2. Virtual Synchronous Generator.....	29
2.1. The basics of VSG concept. Implementations of VSG.....	29
2.2. VSG-C topology.....	42
3. Investigation of VSG-C topology.....	47
3.1. Linearized state-space model of VSG-C.....	48
3.2. Investigation of linearized VSG-C topology response.....	57
3.3. Investigation of detailed non-linear model.....	60
4. Financial management, resource efficiency and resource saving.....	62
5. Social responsibility.....	86
Conclusion.....	99
Sources.....	100

Abstract

The paper contains 104 pages, 30 figures, 24 tables, 49 sources.

Keywords: renewable energy, energy storage systems, power converters, virtual synchronous generators, robustness, modal analysis, small-signal modelling.

Object of study: topology of current-controlled Virtual Synchronous Generator.

Purpose of the work: propose possible solution of the problem of integration of renewable energy-based generation in power systems.

As a result of study the topology of current-controlled Virtual Synchronous Generator was proposed and its positive influence on power system's robustness was proved.

Scope: electric power systems, distributed networks.

Introduction

Decarbonization is the predominant vector of energy development at present. In this context, there has been a continuous increase in the introduction of power generation plants, whose primary energy source is renewable energy, into power systems.

Most of these are connected to the grid through power semiconductor-based devices. They are controlled using the standard approach whereby the grid power converter, an inverter, is the grid-following and a phase locked loop (PLL) is used for synchronization. This implementation results in a reduction in the overall mechanical inertia of the power system and, as a consequence, the problems associated with a significant reduction in frequency and an increase in its rate of change under various perturbations in low-inertia power systems.

In addition, RES operate in the mode of maximum active power generation and practically do not participate in the regulation of the grid regime. As a result, an alternative control paradigm has been proposed to solve these problems, within which the PC becomes grid-forming. Among the existing approaches, the concept of virtual synchronous generator (VSG), which aims to simulate the properties and capabilities of traditional synchronous generation, is considered the most promising and effective.

There is a significant number of different implementations of the VSG, with both strengths and weaknesses. For example, most of the implementations use an PLL, which causes problems in weak and ultra-weak networks, as well as interacting with other similar loops, with the result that the performance of all PLL in the system deteriorates. In addition, most concepts present the synchronous machine model either too much or in insufficient detail, and there is a high probability that the numerical solution will be unstable.

Topology of current-controlled VSG is proposed in this paper due to solve problems mentioned above.

This paper is structured as follows. Section 1 is devoted to an analysis of the main problems in the integration of RES into power systems, as well as a study of possible options for its implementation. Section 2 describes the structure of the most popular VSG topologies, their advantages and disadvantages. The structure of the proposed VSG-C topology is also described. Section 3 is devoted to the mathematical description of the VSG-C topology and the study of its response when it is necessary to participate in the regulation of the network mode. The study is carried out using the Matlab/Simulink software package and the model is verified in the PSCAD software package.

1. Green Energy. Current positions, trends and problems

Green energy (GE) is a set of technologies for generating energy with minimal environmental impact [1]. It is one of the most important and relevant trends in the development of modern power systems worldwide. As one of the methods of solving the problems of global climate change, it has economic potential and several market advantages due to the fact that RES are sold on the local market and are less susceptible to price fluctuations or failures in supply chains [1].

The installed capacity of EGU RES is actively growing. According to IRENA, between 2012 and 2021, the total capacity of EGU-RES in the EPS of the world's largest economies increased from 785 597 MW in 2012 to 1 857 623 MW in 2021 [2]. The dynamics of this change is shown as a bar chart in Figure 1.

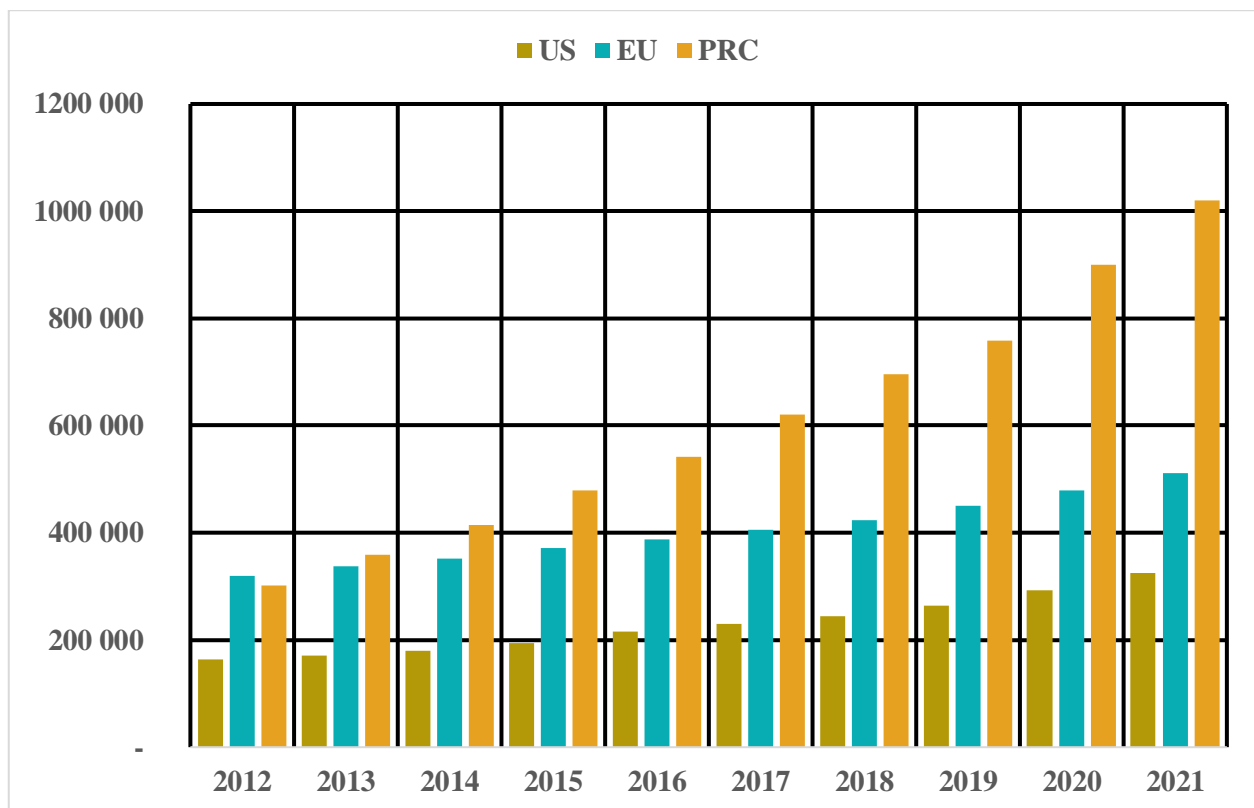


Figure 1 - Change of the total installed capacity of EGU-RES (MW) in EPS of the world's largest economies during the period from 2012 to 2021

In addition to the installed capacity of EGU-RES, the weight of this type of generation is also growing. According to IRENA, between 2012 and 2021, the share of

EGU-RES in US EPS increased from 15.4% to 27.5%, in the EU from 69.3% to 79.6%, and in China from 26.3% to 42.9% [2]. The dynamics of this change is shown as a bar chart in Figure 2.

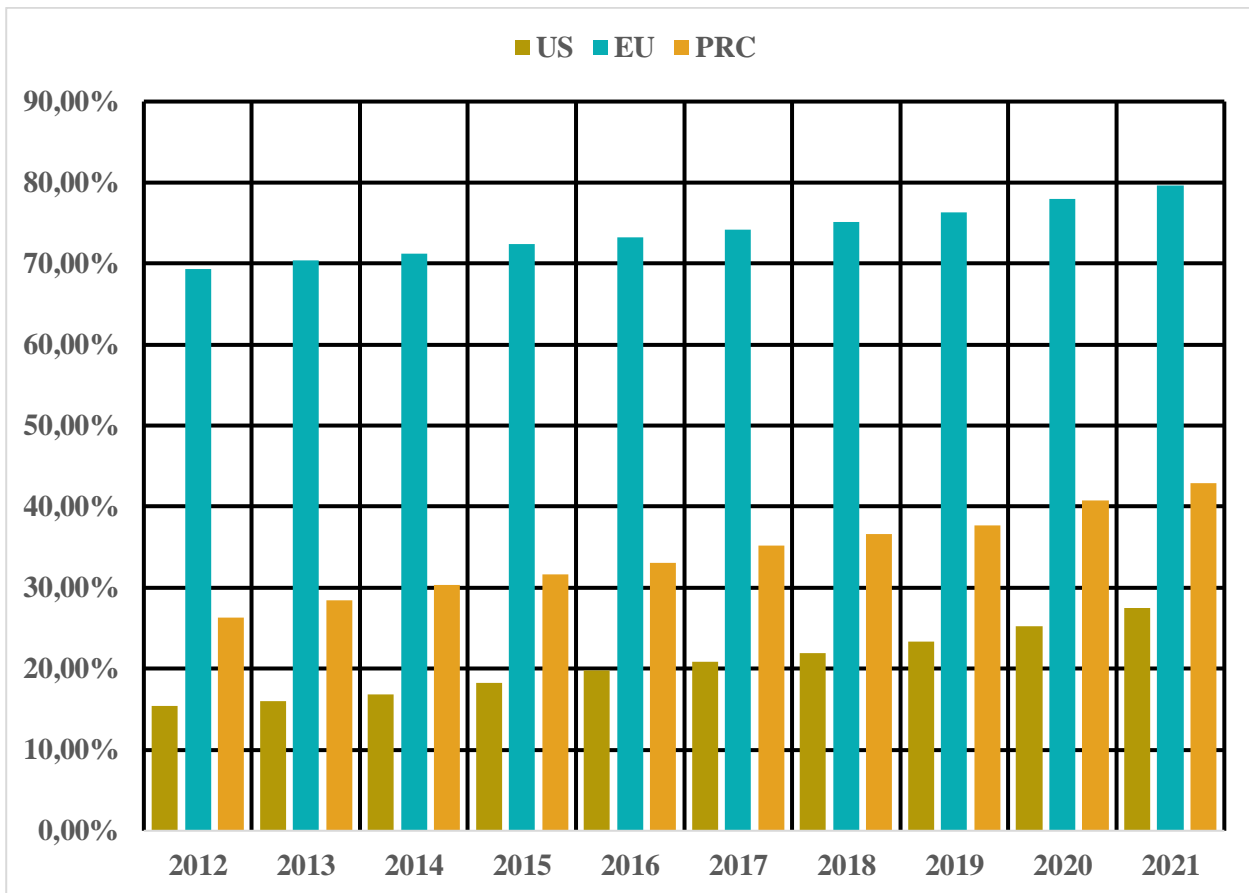


Figure 2 - Change of the share of EGU-RES in the EPS of the world's largest economies from 2012 to 2021

There are five most widespread and rapidly developing types of RES: hydro-power - the most common type of RES, wind energy, solar energy - the fastest growing type of RES, bioenergy and geothermal energy [1]. The vast majority of EGU RES belong to the first three types of RES. A distinction can be made between wind EGUs (WEGUs), solar EGUs (SEGUs) and hydro EGUs (HEGUs). Statistical data [2], presented as bar charts in Figures 3, 4 and 5, allow to estimate the dynamics of the ratio between these types of EGU-RES in the EPS of the world's largest economies.

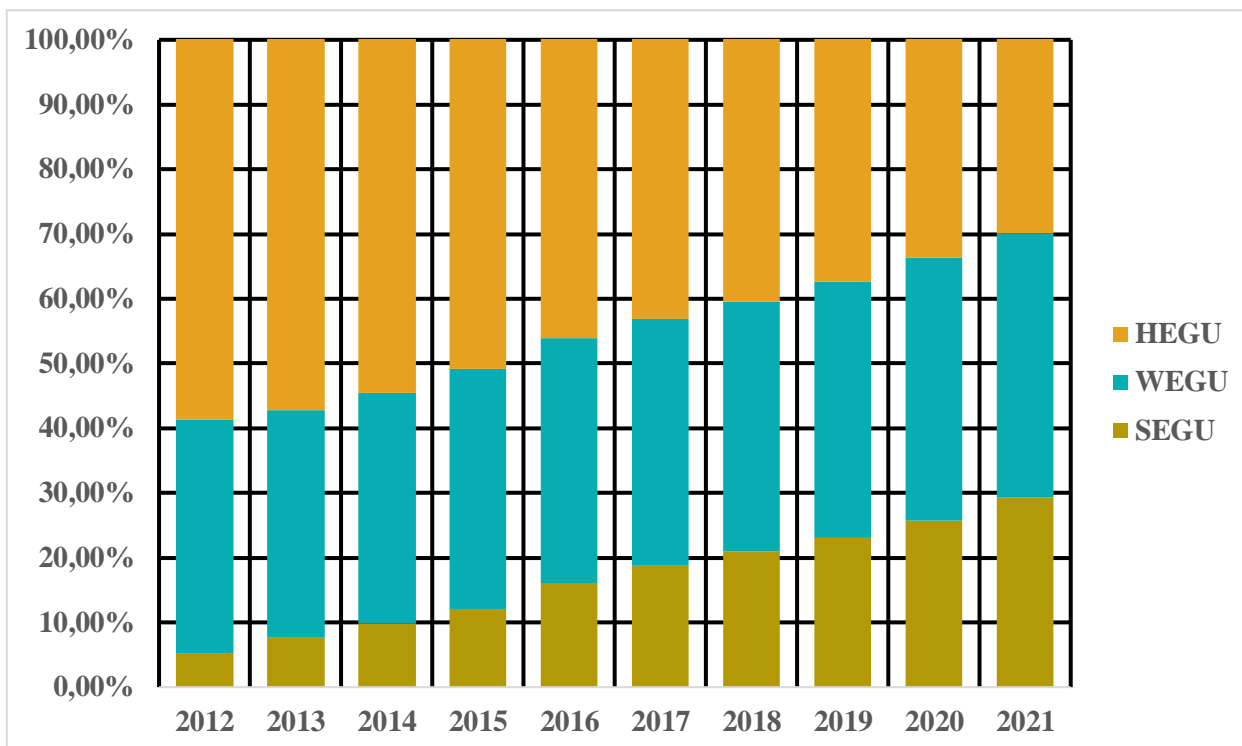


Figure 3 - Dynamics of change in the ratio of the main types of EGU-RES in the U.S. EPS from 2012 to 2021

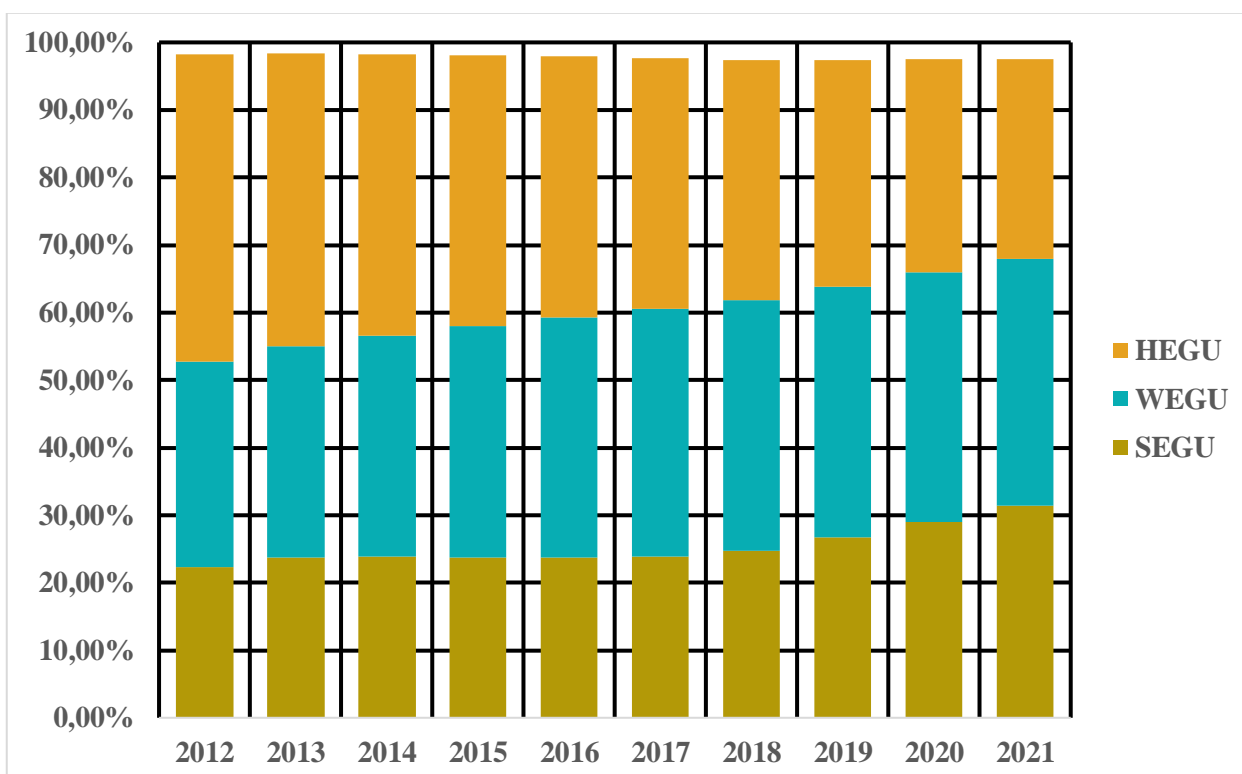


Figure 4 - Dynamics of change in the ratio of the main types of EGU-RES in the EU EPS from 2012 to 2021

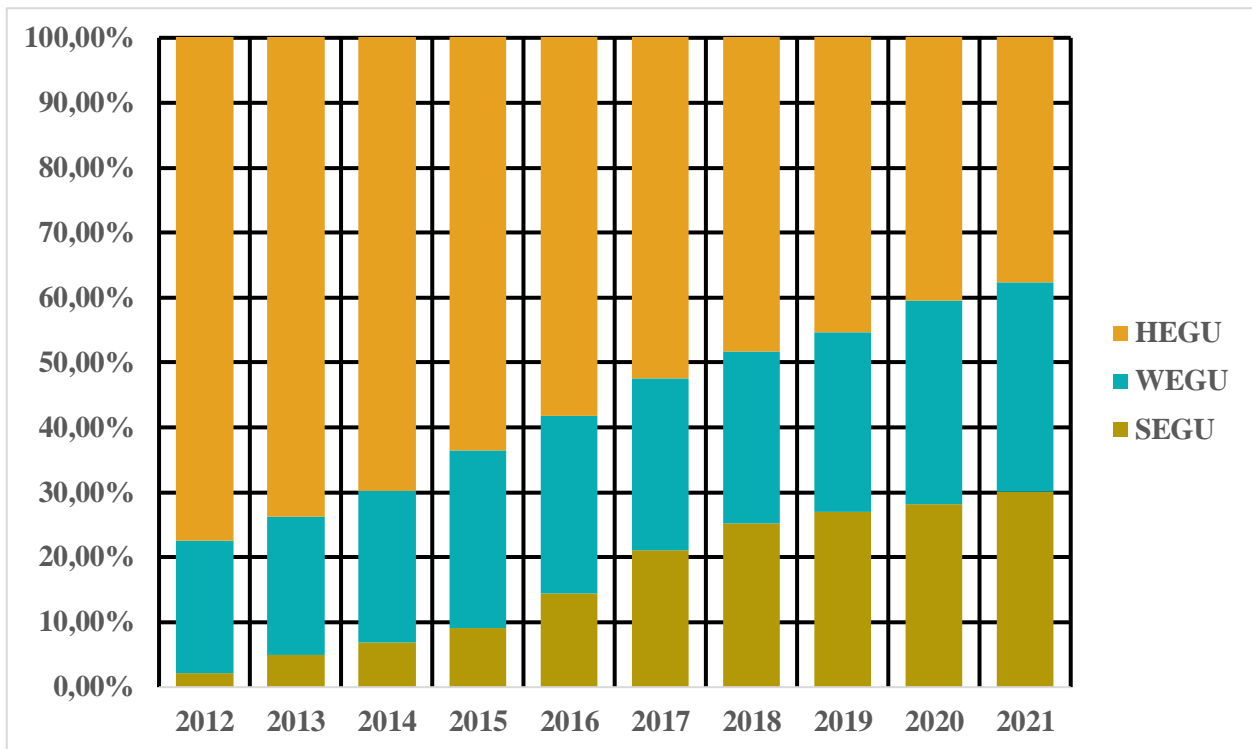


Figure 5 - Dynamics of change in the ratio of the main types of EGU-RES in China's EPS from 2012 to 2021

By 2021, the role of solar and wind in the energy mix of the world's largest economies has increased. At the same time, the share of hydropower, which is more traditional for power systems, in the total installed capacity of EGU RES has decreased. These facts indicate significant changes in the RES structure of the economies analyzed. The ratio between the main types of RES has become more balanced.

The share of RES in Russia's EPS is much lower than in the economies mentioned above. The dynamics of changes in the installed capacity of EGU-RES by types of RES and their weight in the total generation in Russia from 2012 to 2021 can be traced from the statistical data of IRENA [2], which are shown as bar charts in Figures 6 and 7.

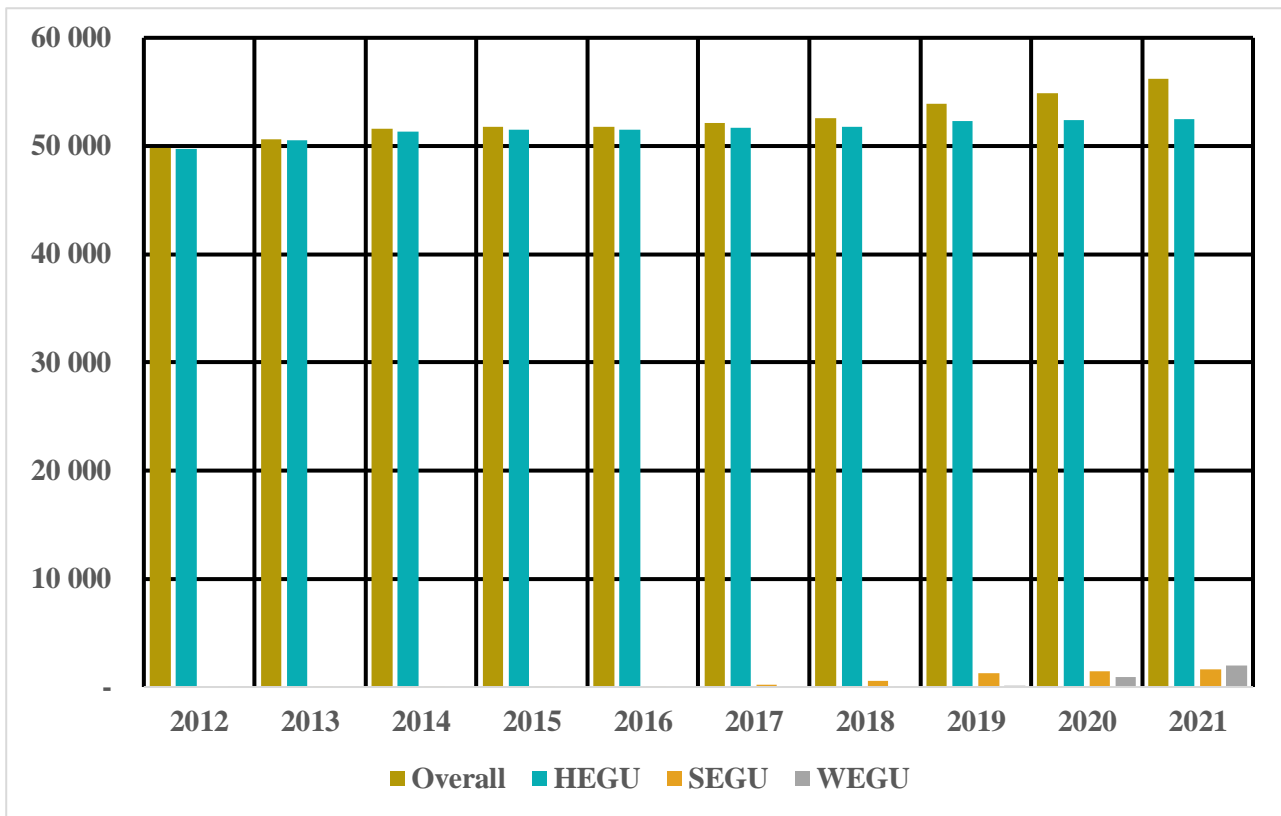


Figure 6 - Change in Installed Capacity of EGU-RES (MW) in the EPS of Russia from 2012 to 2021

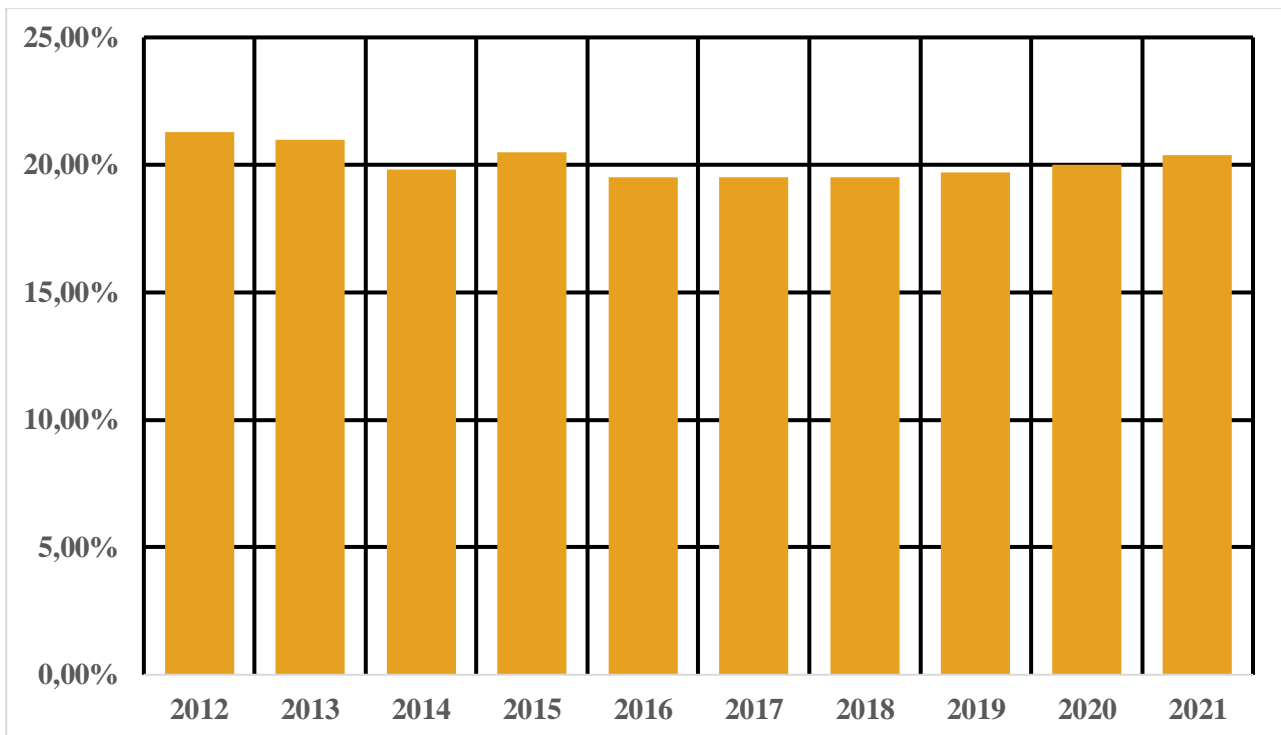


Figure 7 - Change in the share of EGU-RES in the EPS of Russia from 2012 to 2021

Both the installed capacity of EGU-RES and its share in total generation changed insignificantly over the period considered. It is possible to perform a more detailed analysis of the structure of Russian GE on the basis of IRENA data [2], considering the structure of Russian GE in the period from 2012 to 2021.

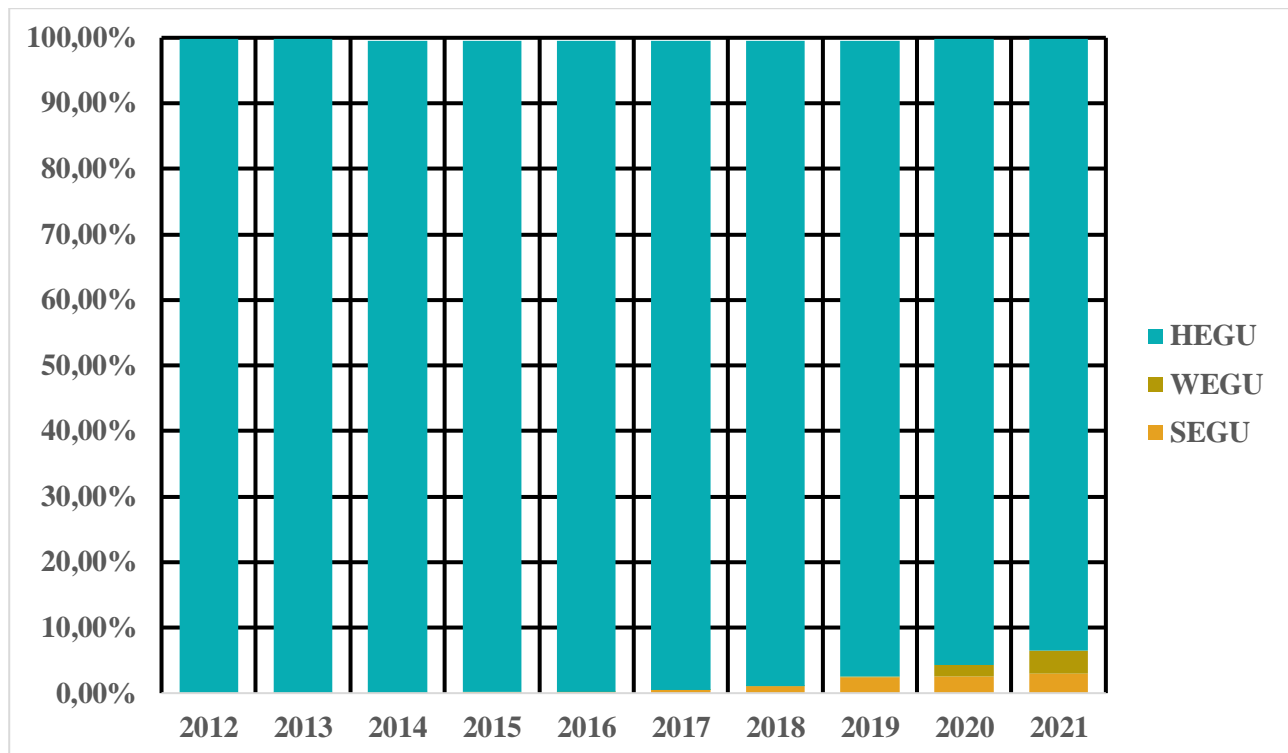


Figure 8 - Dynamics of the structure of Russian GE in the period from 2012 to 2021

This statistic treats the Russian electricity system as a whole. At the same time, an important factor is the length of Russia's UEPS and its division into large parts - Unified Energy Systems (UES). In total, there are seven UES on the territory of Russia: UES of East, UES of Siberia, UES of Ural, UES of Middle Volga, UES of South, UES of Center, UES of North West[3]. The structure of power generation in each of these systems is different. The share of generation types within each of Russia's UES as of 01.01.2022 is shown in Figure 9 in the form of bar charts based on open data from JSC "System Operator of the Unified Energy Power System" and the Ministry of Energy of the Russian Federation [4].

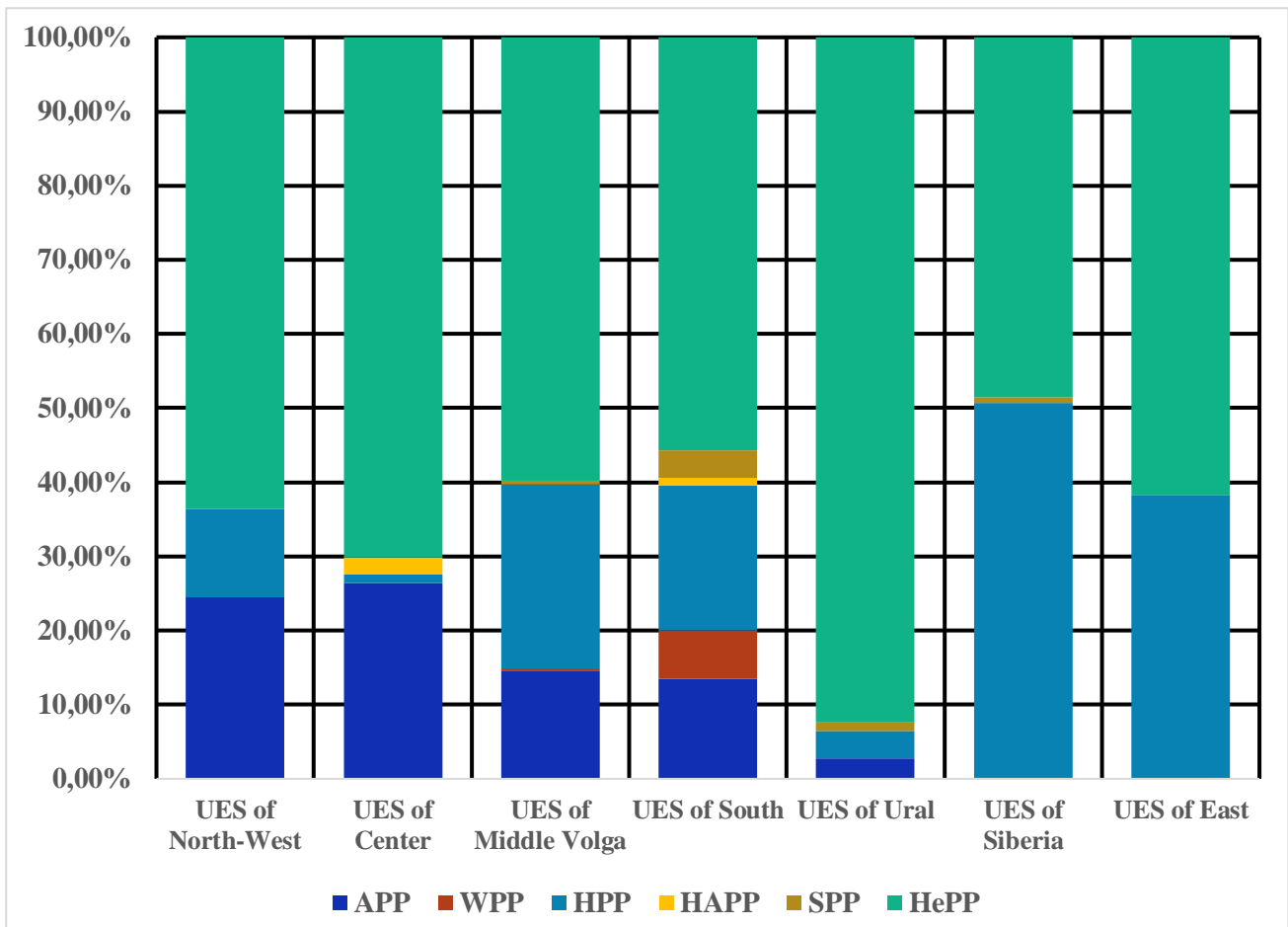


Figure 9 - Relationship between types of power generation within each of the UES of Russia as of 01.01.2022

The predominant type of power plants is coal-fired TPPs. Their share in the total installed capacity of the UES varies from 48.55% in the Siberian UES to 92.38% in the Ural UES. Among the RES significant positions are occupied by traditional for the energy sector HPPs, which corresponds to the statistical data of IRENA [2], shown in Figure 8. Against the background of other UES, the generation structure of South UES stands out, being the only UES in the UEPS of Russia, the share of alternative RES - in this case it is WEGU and SEGU - in which has a relatively high value - 10.11%. Small capacities are also present as part of the Ural UES - 1.22% corresponding to SEGU, Siberian UES - 0.76% SEGU and Mid-Volga UES - 0.50% SEGU and 0.39% WEGU. Thus, despite the small all-Russian indicators, the composition of the UEPS of Russia includes UES with a relatively high share of alternative RES, the installed

capacity attributable to them is increasing significantly compared with the indicators of previous years, starting from 2017.

The above data indicate the growth of the installed capacity of EGU associated with alternative RES – WEGU and SEGU, both in the world's largest economies, and in the Russian Federation. Speed, volumes and uniformity of this process are different, but the trend is noticeable and it affects the development of the world power industry, raising the problem of integration of growing volumes of EGU-RES capacity into power systems, relevant to WEGU and SEGU due to the fact that HEGU are traditional RES and are an integral part of power generation and maintaining stability of the ES.

Wind EGU, in accordance with the standard of the International Electrotechnical Commission (IEC) for the definition of common (standard) dynamic models for WEGU [5] and the position of the international organization IEEE (Institute of Electrical and Electronics Engineers) [6], are classified by the type of electrical machine used in their topology. In this classification there are four basic types, the topology of each of them is shown in Fig. 10.

Wind turbines of type A contain an asynchronous generator (AG) with a short-circuited rotor, the speed of which is limited by the speed of rotation of the blades, and the possibility of response to changes in wind speed is insignificant. The installation of power converters (PC) or any other devices for regulating the generator speed is not provided in this type of wind turbine [7].

Wind turbines of type B also contain AGs, but unlike wind turbines of the type A, AGs with a phase rotor are used, and a variable resistance is included in the rotor circuit to control the speed of rotation. This type of WEGUs are controlled more flexibly, but they have relatively high electric losses and very limited response to the network requirements [7].

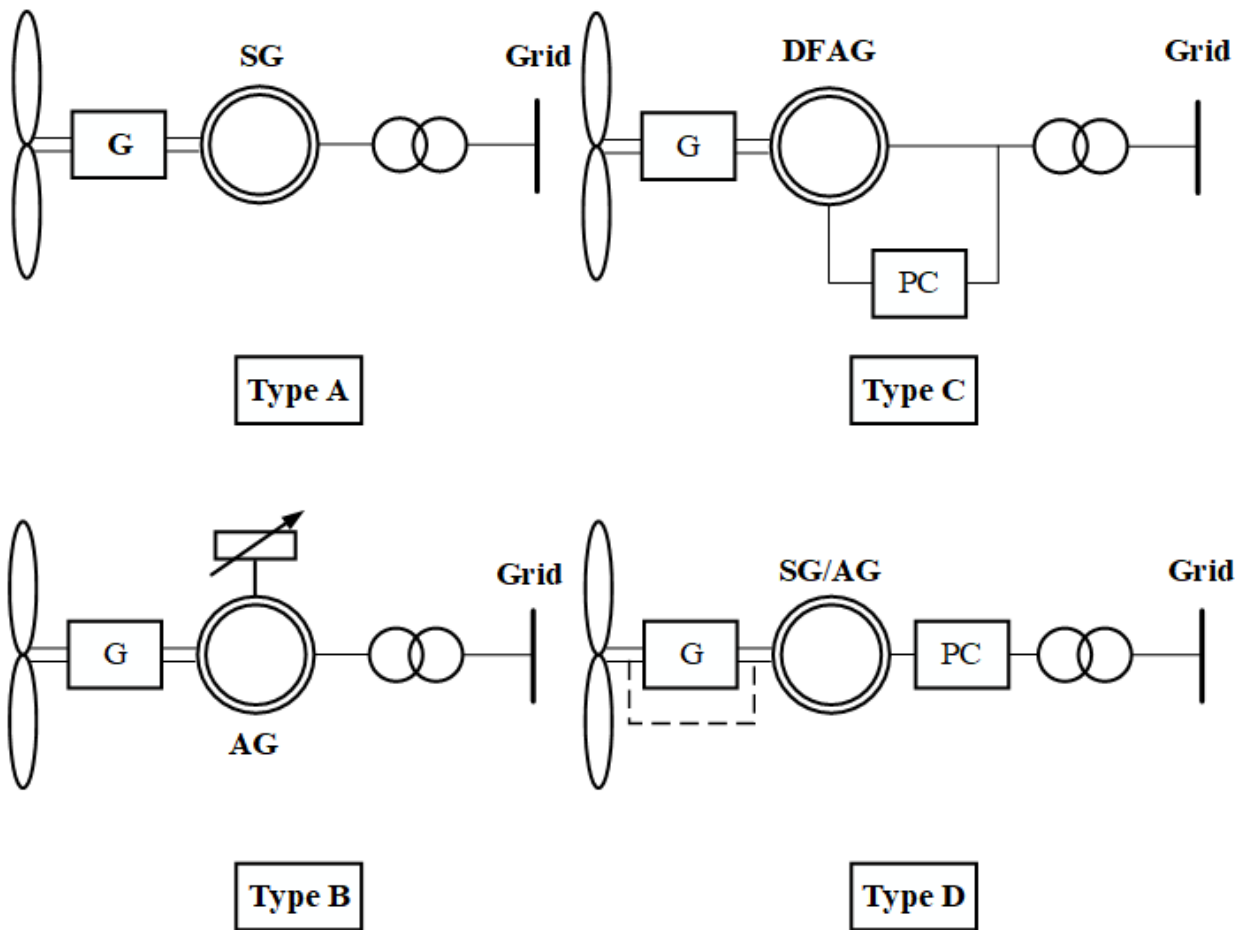


Figure 10 - Topology of the main types of wind turbines (G-gearbox, PC - power converter, AG - asynchronous generator, DFAG – double-fed asynchronous generator, SG - synchronous generator)

The type C of wind turbines uses asynchronous double-fed asynchronous generators (DFAG), which are phase-rotor AGs whose rotor circuits are fed externally. In this case, the rotor circuits are fed through the PC, which provides high controllability, lower losses and improved response to grid demands. Since the SP is only included in the rotor circuits, it affects about 30% of the energy produced by the wind turbine [7].

Type D wind turbines are connected to the grid through PC, and in the design are used gearless wind turbine, coupled with the rotor of synchronous generator, performed either on permanent magnets, or with electric exciter. This feature makes it possible to decouple the wind turbine from the system frequency and control the output

voltage frequency in a wide range, thus reducing its dependence on the stochastic nature of the wind [7].

In [7] an extended classification of wind turbines is proposed: two new types are added – the fifth and the sixth. However, their topology repeats that of the type D, and the main difference lies in the electric generators used: unlike the type D type E uses a synchronous generator rotor coupled to a gearbox, while type F uses an asynchronous generator also coupled to a gearbox. The types under consideration are connected to the mains via a PC, which for the purpose of this work allows them to be included in the fourth type.

Statistics show that the most widespread topology of wind turbines used in power plants is type D - they account for over 35% of the installed capacity of wind turbines in the world [8]. Statistical data [7] show gradual abandonment of the types A and B of WEGUs all over the world - thus, among WEGUs types C and D prevail, and the share of the latter tends to grow and may become the most common WEGU topology in the future [7].

According to IRENA [2], the overwhelming majority of the installed capacity is represented by solar panels: their share in the total installed capacity of global SEGUs during the period from 2012 to 2021 exceeded 97%, reaching its highest value in 2021 - 99.25%. Thus, considering the fact that the installed capacity of EGU-RES is growing and that the share of WEGU and SEGU in them is also increasing, while the majority of them are connected to the grid via power converters, there is a tendency for significant capacities that are not directly connected to the grid to be integrated into power systems and replacing traditional power system generation types.

The electrical decoupling of the wind turbine generated power from the EPS eliminates the relationship between generator speed and grid's frequency [9], as defined by expression (1.1):

$$2 \cdot T_J \cdot \frac{d\omega}{dt} = P_G - P_L \quad (1.1)$$

In this formula T_J – generator’s inertia constant, ω – angular speed of the generator’s rotor, P_G – generated active power, P_L – active power that is consumed by the load.

The exclusion of this relationship eliminates the natural contribution of the generator to the overall system inertia [9]. As traditional generating capacities are replaced by green ones, this feature may lead to a significant reduction in equivalent inertia constant of the power system [8], which follows from expression (1.2):

$$T_{J,EPS} = \frac{\sum_{i=1}^n T_{Ji} \cdot S_i}{S_{EPS}} \quad (1.2)$$

In this formula T_{Ji} and S_i – inertia constant and rated power of i^{th} generator, n – number of grid-connected generators, S_{EPS} – overall EPS power that is equal to the rated power of all working generation units [8].

According to (1.2), as the number of EGU-RES connected to the system increases, the value of S_{EPS} will also increase, while the numerator will remain the same, due to the extremely small values of T_{Ji} of each EGU-RES. The value of the equivalent inertia constant $T_{J,EPS}$ will decrease accordingly. This dependence can also lead to more frequent changes in the inertia constant, compared to conventional power systems, caused by fluctuations in the power produced by the EGU-RES due to changes in wind speed or solar radiation intensity.

As traditional generation types are replaced by alternatives and the consequent significant change in the dynamic properties of the EPS appears, it becomes more acute, the applicability of conventional methods of preventing instability - fast automatic control systems for generator excitation, pulse turbine unloading, generator/load part shutdown, etc. - becomes more critical.

Power converters - inverters that connect the EGU-RES to the grid - can be a solution to the problems mentioned above. They are a source of output voltage for the EGU-RES, the parameters of which can be controlled. Broadly speaking, inverters can be classified as grid-following (GFL) and grid-forming (GFM) [10].

GFL inverter control systems are based on phase and amplitude of grid voltage signals. These are monitored using a phase locked loop (PLL) which measures at the connection point, referred to in the literature as a common coupling point (CCP). In this way, synchronization with the grid is achieved and the GFL inverters follow its phase, functioning as controlled current sources [11]. The output power of a GFL inverter is generally determined via static characteristics based on the measured grid's voltage amplitude and frequency [10]. The output power is regulated by controlling the output currents and neither the amplitude nor the frequency of the output voltage can be controlled independently as this requires an additional voltage source [11]. This power inverter control strategy is the convenient and most common for EGU-RES [11, 13]. The schematic diagram of the GFL inverter is shown in Figure 11.

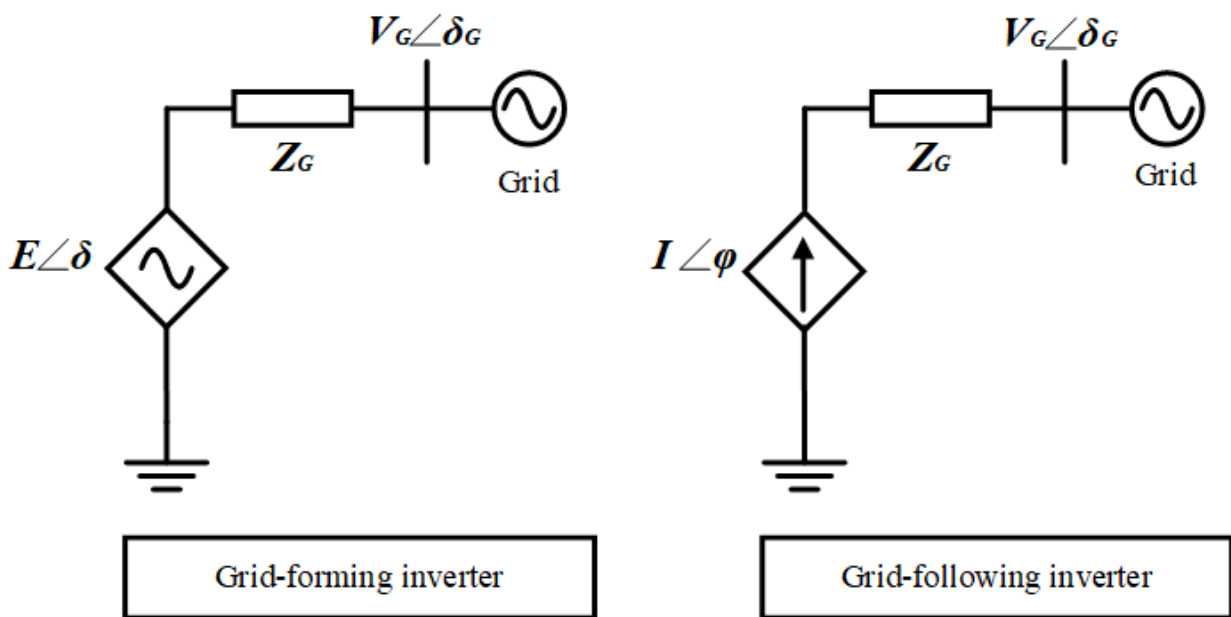


Figure 11 – Circuit diagrams of GFM and GFL inverters

A schematic diagram illustrating the general principle of a power converter GFL control system is shown in Figure 12. This system consists of three main parts [12]:

1. Active and reactive power control. The inputs of this part are the differences between the instantaneous values of active and reactive powers flowing into the CCP (p and q respectively) and the instantaneous values of active and reactive powers

flowing into/from the system (p^* and q^* respectively). The power values are calculated based on the measurement of currents and voltages on the PC side and on the grid's side.

2. Grid's voltage phase detection. For this PLL is used. Its inputs are the three grids voltage phases v_{gabc} measured in the CCP. The output values of this loop are the calculated frequency $\widetilde{\omega}_g$ and angle $\widetilde{\theta}_g$ of the mains voltage. They should be as close as possible to the actual values, reflecting the actual state of the grid's voltage. For this purpose, a PI controller is included in the structure of PLL. The PLL circuit diagram is shown in Figure 13.

3. Generation of the output control signal for the PC based on previous calculations.

GFM inverters, unlike GFL inverters, are able to control the frequency and amplitude of the output voltage. On this basis, GFM inverters can be thought of as a controlled voltage source [10]. However, there is no general principle for GFM inverter control systems. There are many possible variants of the implementation of this control strategy for PC, and many of them have significant differences in structure and construction principle. The most common are strategies based on control based on droop characteristics, as well as those based on the concept of a virtual synchronous generator (VSG), and the latter group is the most promising in the near future [13].

The VSG concept is based on the idea of the inverter simulating the behaviour of a Synchronous Generator (SG) by incorporating SG equations into the control algorithms. Such SPs have a number of advantages. For example, they are capable of providing a number of EPS support services: increasing the system strength, implementing a tunable inertial response, and quickly adjusting the output voltage amplitude and frequency [13].

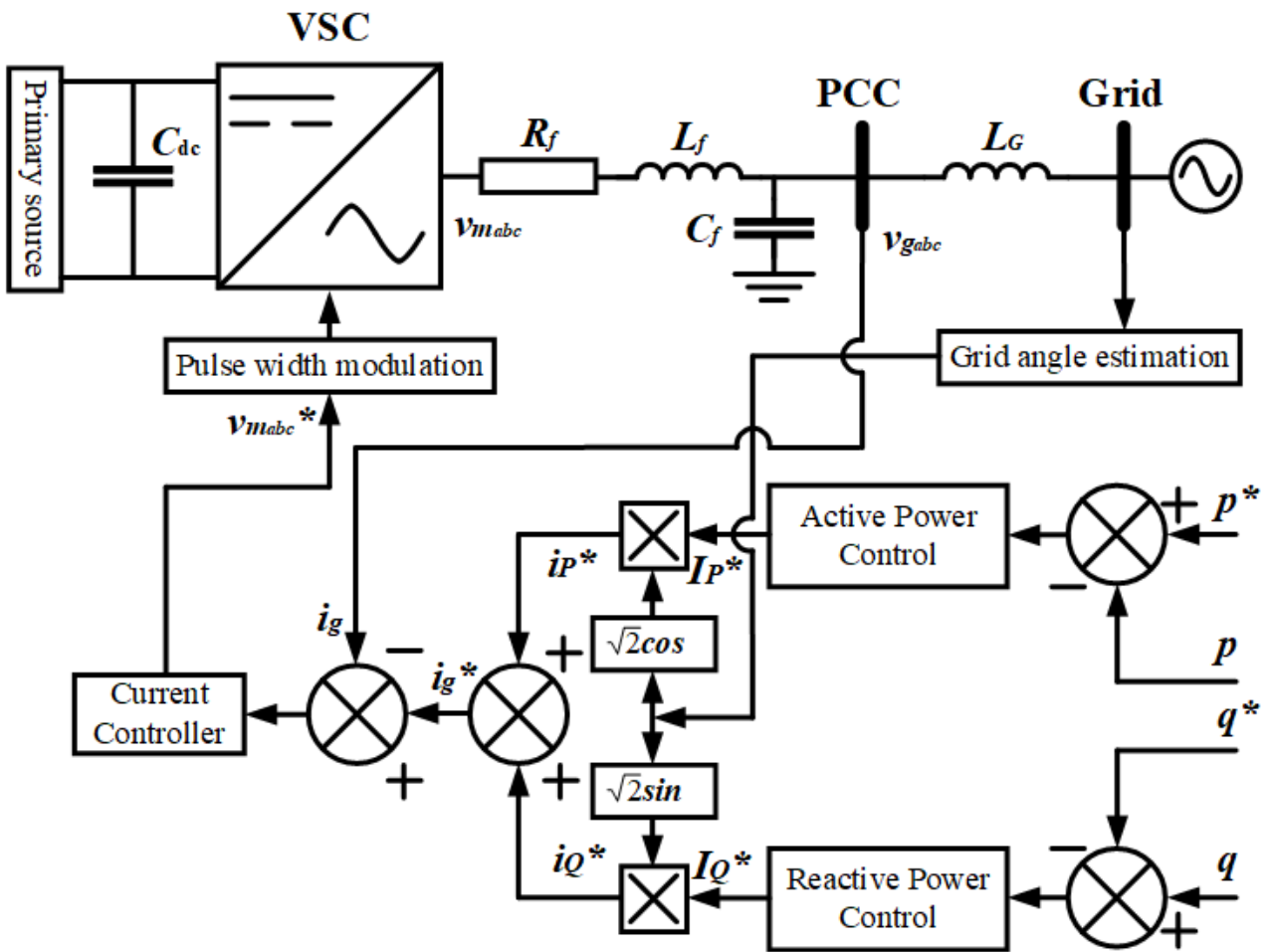


Figure 12 - Schematic diagram of the general principle of the inverter slave control system

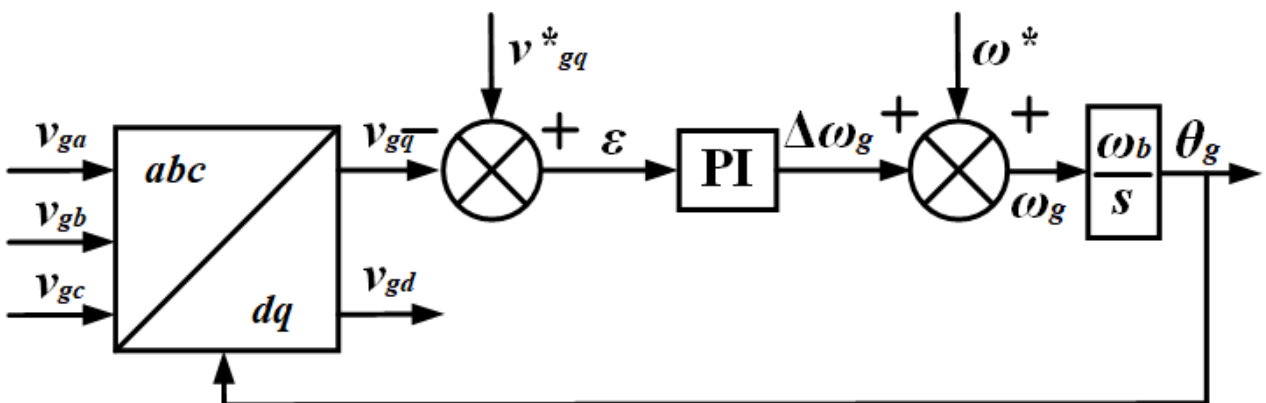


Figure 13 - PLL circuit diagram

At the same time, VSG inverters are capable not only of simulating traditional SGs, but can significantly improve the dynamic properties of the EPS, as the control system parameters are not limited by the design of a particular machine and can be changed to achieve the required transient response [13].

2. Virtual Synchronous Generator

2.1. The basics of VSG concept. Implementations of VSG

The VSG is a control algorithm that organizes the interaction of the EGU-RES, energy storage systems (ESS), and power electronics so that the output voltage of the inverter simulates the response of the synchronous generator [14]. The block diagram describing the basic principle of the VSG model is shown in Fig. 14 [15].

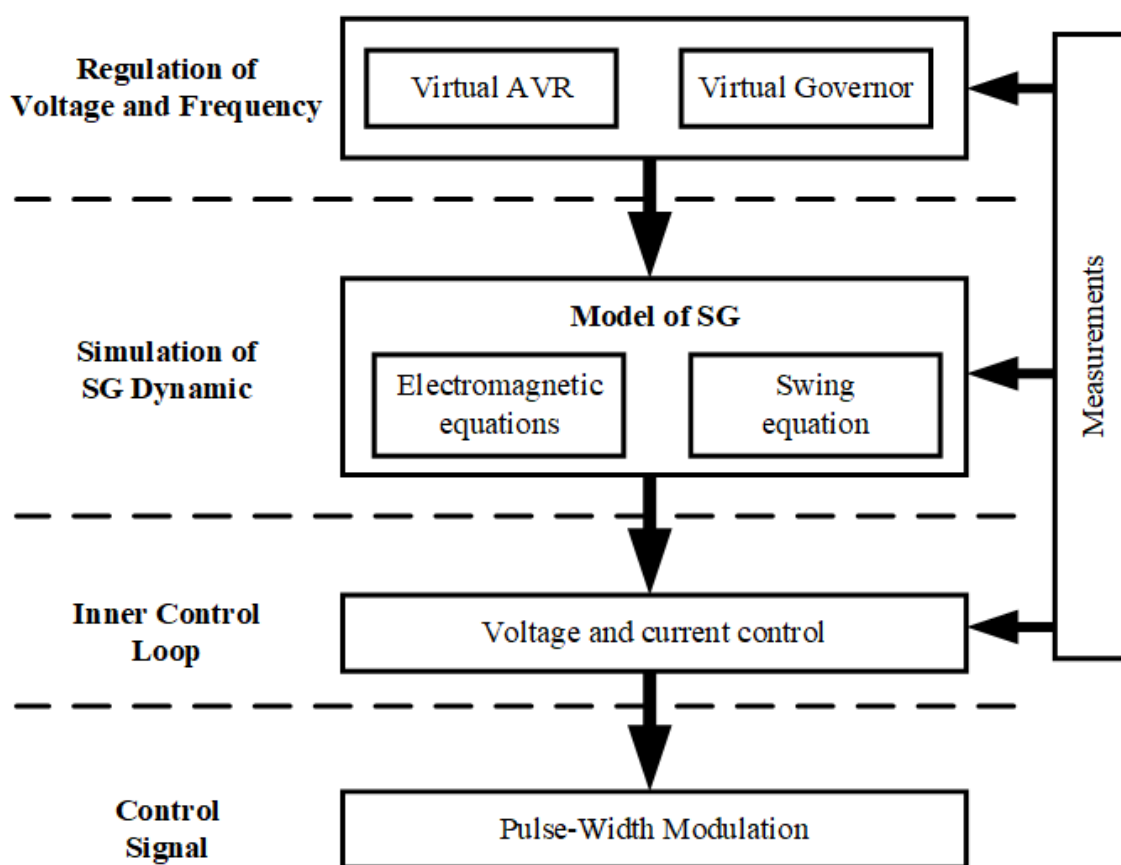


Figure 14 - Basic principle of VSG

This principle can be divided into five parts: a unit for measurement and calculation of input quantities (active and reactive power flows into the network, voltage amplitude and phase in CCP, network voltage amplitude and phase), a unit for simulation of AVR and ASR systems (or an external control loop), a unit for simulation of synchronous generator dynamics, an internal control loop and a control signal generation unit.

The role of the external control loop is to regulate the voltage amplitude (virtual AVR system) and frequency (virtual ASR system) by analogy with AVR and ASR systems in traditional SGs [15]. Different implementations of frequency regulator are possible, the best response is demonstrated by the regulator with droop characteristics. The virtual AVR model is usually a proportional-integral control, either voltage, with reactive power droop, or reactive power, with voltage droop [15].

The dynamic processes of a synchronous machine are described using the swing equation and a system of electromagnetic equations of various orders of the synchronous generator. In addition to the accuracy of the description, these models differ in their effect on the response of the VSG [15]. So, the 7th order detailed model of SG can reduce the rate of change of frequency. At the same time, the 2nd order model has a similar frequency nadir, but it provides no threats of synchronous resonance and instability of the numerical solution. The 2nd order model is the best option for handling electromagnetic processes in synchronous machines, which is due to the elimination of excessive informativity while maintaining sufficient efficiency by changing the virtual stator winding resistance. However, due to their simplicity, models that exclude electromagnetic processes in the synchronous machine are the most common [15].

The internal control loop has a significant influence on the dynamics of the whole VSG model. This loop can be implemented in three variations, depending on the input reference values. This allows one to differentiate between current-, voltage- and power-controlled models of a VSG. These circuits are usually based on PI controllers in a three-phase system, which have several advantages, the most important of which is the ability to implement current limiting algorithms. At the same time, a significant disadvantage is the possible instability of the numerical solution - especially in the case of a high-order SG model - due to the properties of PI controllers. Thus, this loop makes the whole VSG structure extremely sensitive to the chosen solution method and integration step [15].

The final VSG control signal is generated by pulse-width modulation (PWM) based on the results of the internal control loop calculation.

In spite of the common fundamentals of the VSG concept, its implementation can be very different. Thus, within the VSG concept, there are many variants of control systems. The authors of review articles highlight such VSG topologies as VISMA and IEPE [14, 15, 16, 17], Synchronverter [14, 15, 16, 17], ISE Labs topology [14, 16, 17] and VSYNC [15, 16, 17]. Each of these topologies will be discussed below.

VISMA and IEPE

The VISMA (Virtual Synchronous Machine) topology has three implementations [15]: VISMA [18], VISMA-Method 1 (VISMA 1) [19] and VISMA-Method 2 (VISMA 2) [19]. All three implementations include both mechanical and electromagnetic parts of the synchronous machine, but VISMA has the most detailed model of electromagnetic processes, describing in dq-coordinates the processes in the stator winding, damper winding and exciter, and considering the hysteresis phenomenon [18].

VISMA 1 is a simplified implementation of VISMA. The electromagnetic processes in the SG are described by a model that considers the stator winding voltages, the inertia is considered via the swing equation [19]. Also, the phenomenon of hysteresis is considered and implemented with a separate controller located structurally before the PWM. The structure and block diagrams of VISMA 1 are shown in Figure 15 [19].

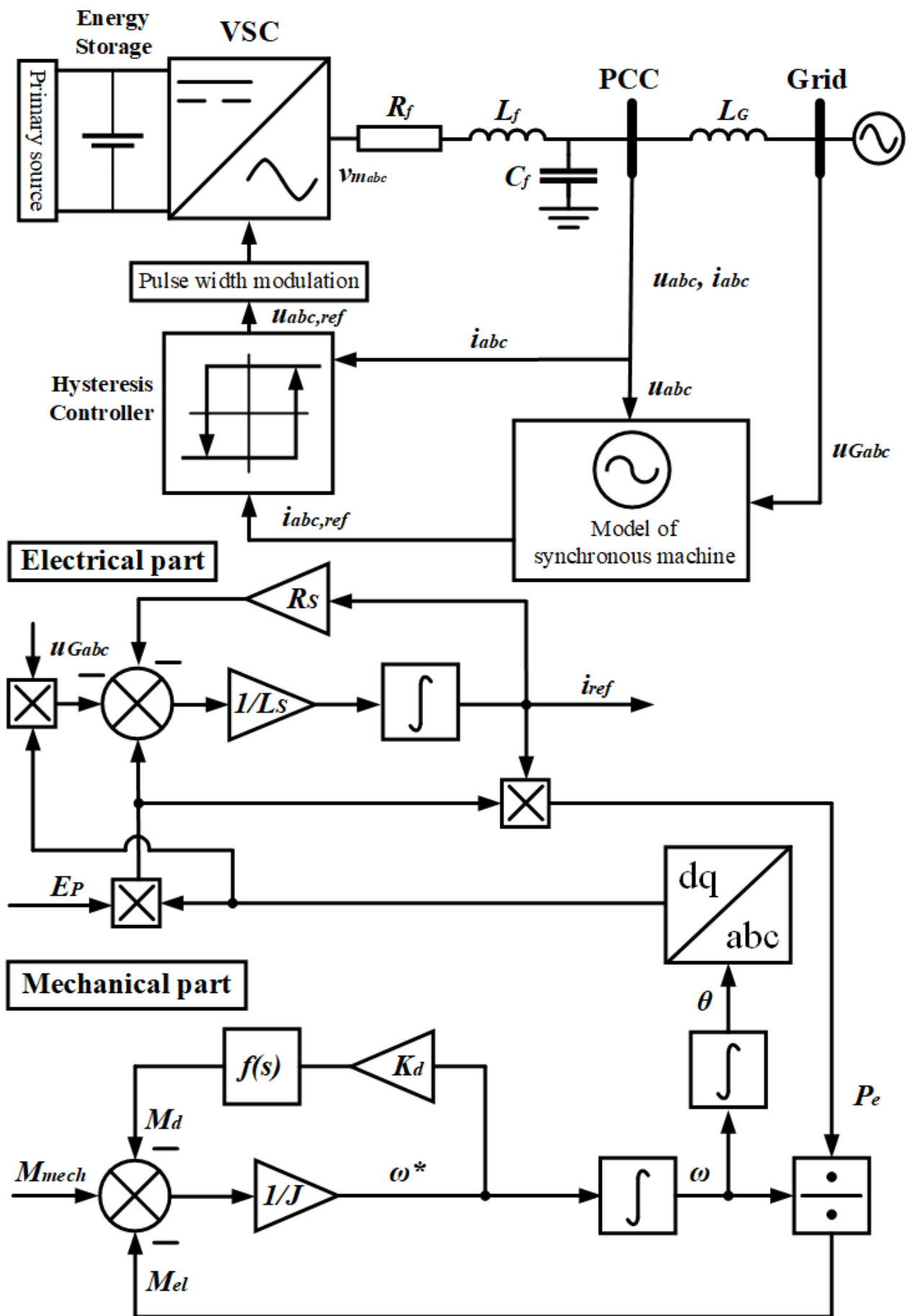


Figure 15 - Structural and block diagram of VISMA 1 topology

For this topology to function, the phase currents and voltages in the CCP as well as the grid's voltages must be measured. The mechanical and electromagnetic models are interrelated: the angle θ is derived from the equation of motion and the current reference i_{ref} is calculated from the stator winding equations to calculate the instantaneous power value and consequently the electrical torque required by the equation of motion.

VISMA 2 and the topology developed by the IEPE (Institute of Electrical Power Engineering) are identical. As in VISMA 1, the electromagnetic processes in the SG are described by 2nd order model. The main difference are the inputs of the model: in VISMA 1, they were voltages in the CCP and in VISMA 2 (IEPE), they are currents [19]. This difference causes the use of differentiation in the model, which may lead to instability of the numerical solution. A low-pass filter is used in the model to increase the stability [19]. A structural and block diagram of VISMA 2 (IEPE) is shown in Figure 16 [19].

The main disadvantages of all the VISMA implementations are the possible instability of the numerical solution due to application of integration and differentiation, which makes them sensitive to the choice of solution method and integration step [16]. The presence of PLL that is used for initial synchronization with the network introduces additional nonlinearities, has complicated parameter settings and also creates a problem of interaction with other PLL loops in the system [20]. A disadvantage of VISMA 2 is the need to limit the transient currents occurring during the mains synchronization period [16].

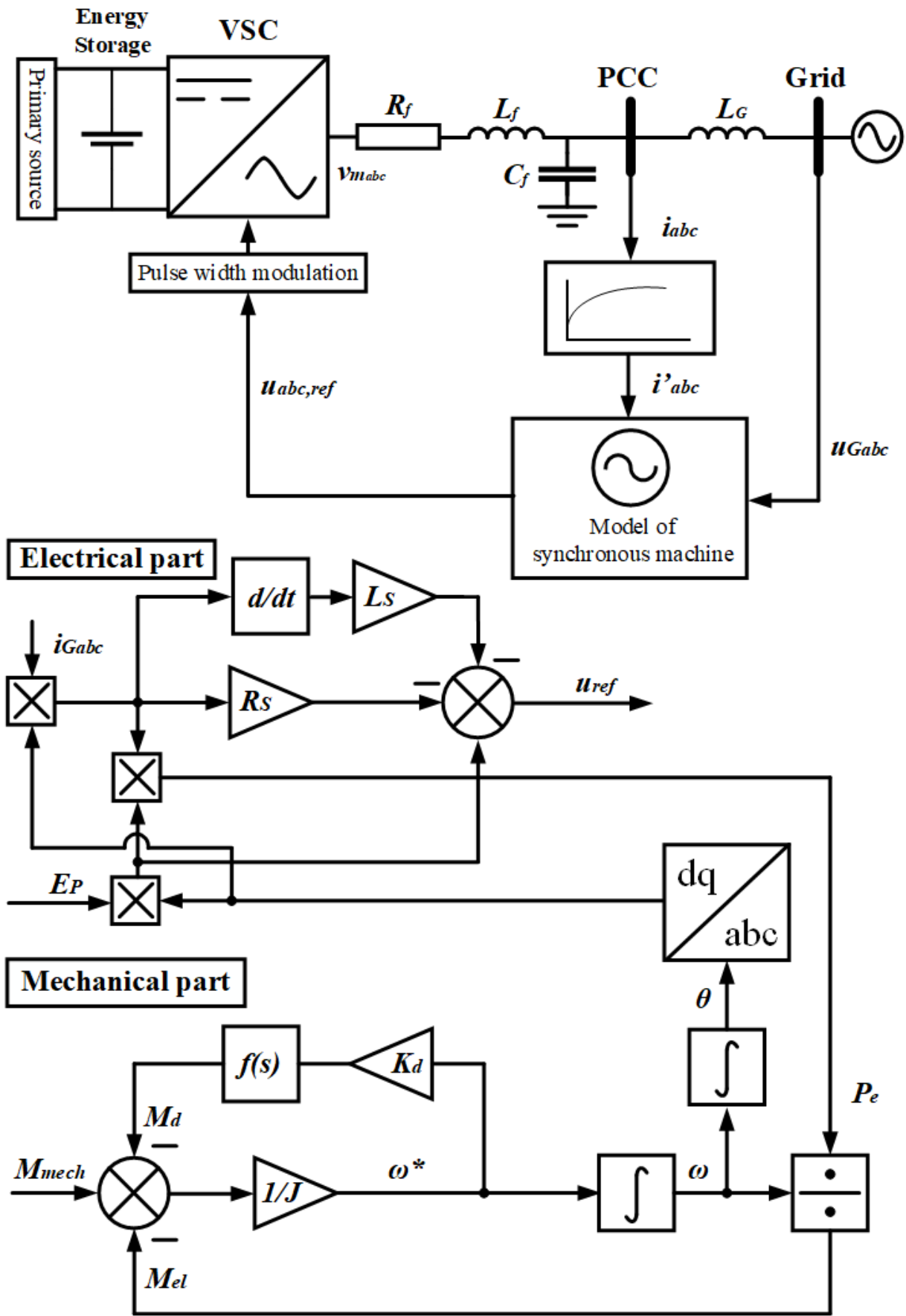


Figure 16 - Structural and block diagram of VISMA 2 (IEPE) topology

Synchronverter

In contrast to all implementations of VISMA, the inputs for the Synchronverter topology are both currents and voltages in the CCP. Another difference is the structure of the electromagnetic process in the synchronous machine model: in Synchronverter, the voltage drops in the stator windings are not considered, but the electromagnetic torque, reactive power and EMF are calculated [20, 21]. Thus, the modulating signal at the PWM input is a vector of EMF, not voltage. The PLL [16, 20, 21] is used for initial synchronization with the grid's voltage.

The mechanical part in this topology is represented by the swing equation, in which an ASR system is simulated via the droop coefficient D_p [21]. The AVR system is represented by a more complex model, in comparison to other topologies, whose output is the exciter magnetic flux [21]. The values of VSG voltage frequency ω_{VSG} and angle θ , excitation flux $M_f i_f$ calculated by these loops as well as the phase currents measured in the CCP are used to calculate the SM electromagnetic processes in the model. Thus, the values of reactive power Q , electromagnetic torque T_e , and EMF reference value necessary for topology operation are formed. EMF reference along with the angle θ are input signals for the PWM block.

The Synchronverter structure and block diagram are shown in Figure 17 [16, 20, 21].

The exclusion of differentiation operation from the calculations is an advantage of this topology, which reduces the output signal noise and increases the solution stability. At the same time an important role in considered topology is played by integrating operation as well as nonlinear functions used in calculations of electromagnetic processes in synchronous machine due to which the instability probability of numerical solution remains rather high [16]. Application of PLL in this topology causes disadvantages similar to VISMA topology.

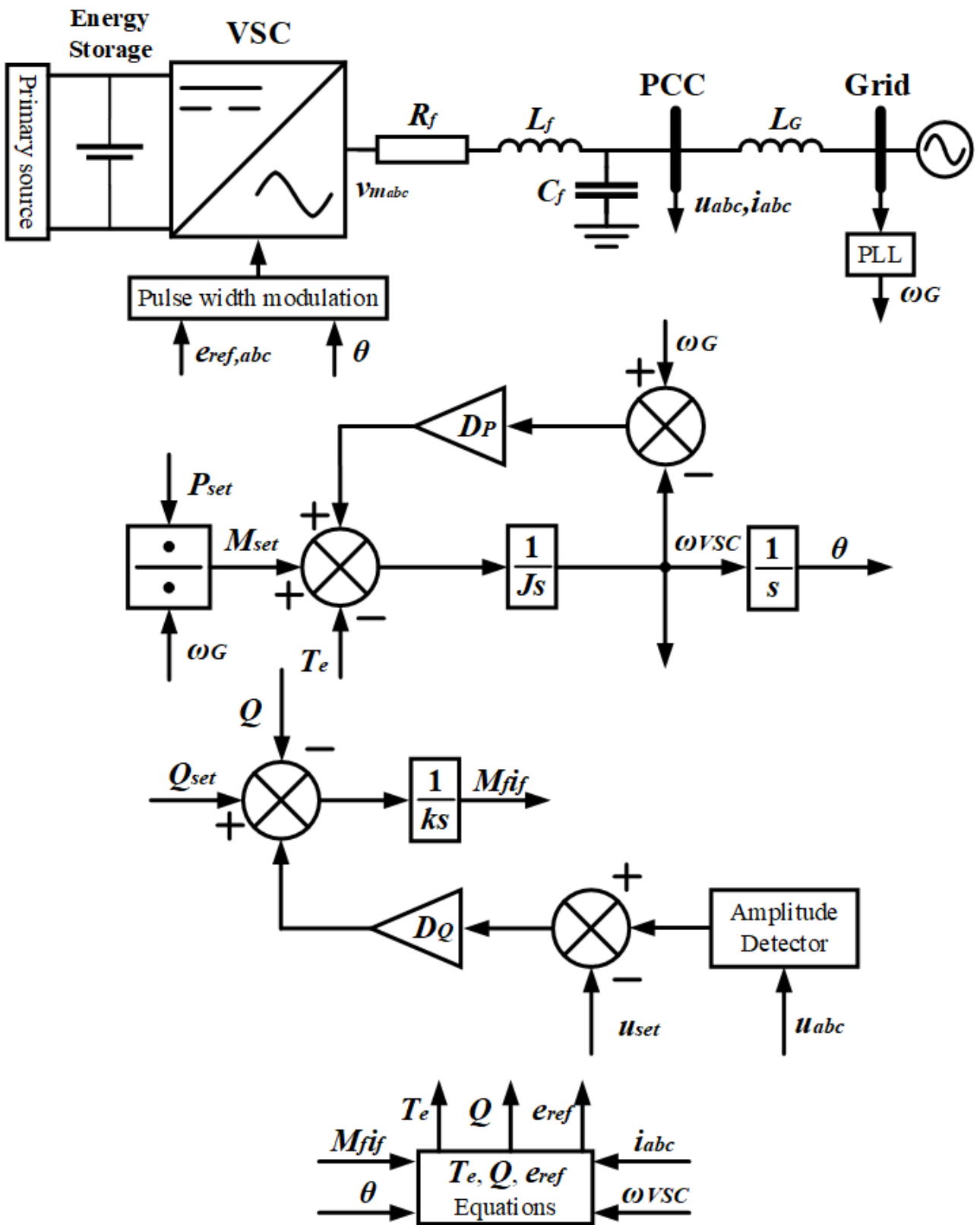


Figure 17 - Structure and block diagram of Synchronverter topology

ISE Labs topology

In contrast to VISMA (IEPE) and Synchronverter topologies, the topology developed by ISE Labs does not contain a model of the electromagnetic processes in the synchronous machine. Thus, only the mechanical processes as well as the operation of the AVR and ASR systems are represented.

The inputs of this topology are the instantaneous values of the active and reactive powers in the CCP, calculated from the measured phase currents and voltages in the CCP, as well as the frequency in the network required for initial synchronization with the network and measured by the PLL [16].

The AVR system in this topology is implemented in a simplified way, through the K_Q droop factor [17]. At the same time the ASR system is made more complicated than in most topologies: in contrast to the frequency droop, here a transfer function is used that considers the controller time constant and its droop. Thus, the model of the mechanical part becomes closer to the real processes [16].

The disadvantages of this topology are sensitivity to the accurate tuning of parameters [16], the probability of instability of the numerical solution due to the introduction of an additional transfer function of the ASR controller. This function makes the tuning process of the topology algorithm more complicated and also increases the rate of change of frequency and its nadir [16]. Besides, reliability of the topology decreases as the PLL is implemented, as well as in previous topologies, and currents in CCP are used as input quantities that causes the necessity of their limitation during initial synchronization with the grid.

The structural and block diagrams of this topology are shown in Figure 18 [14, 16, 17].

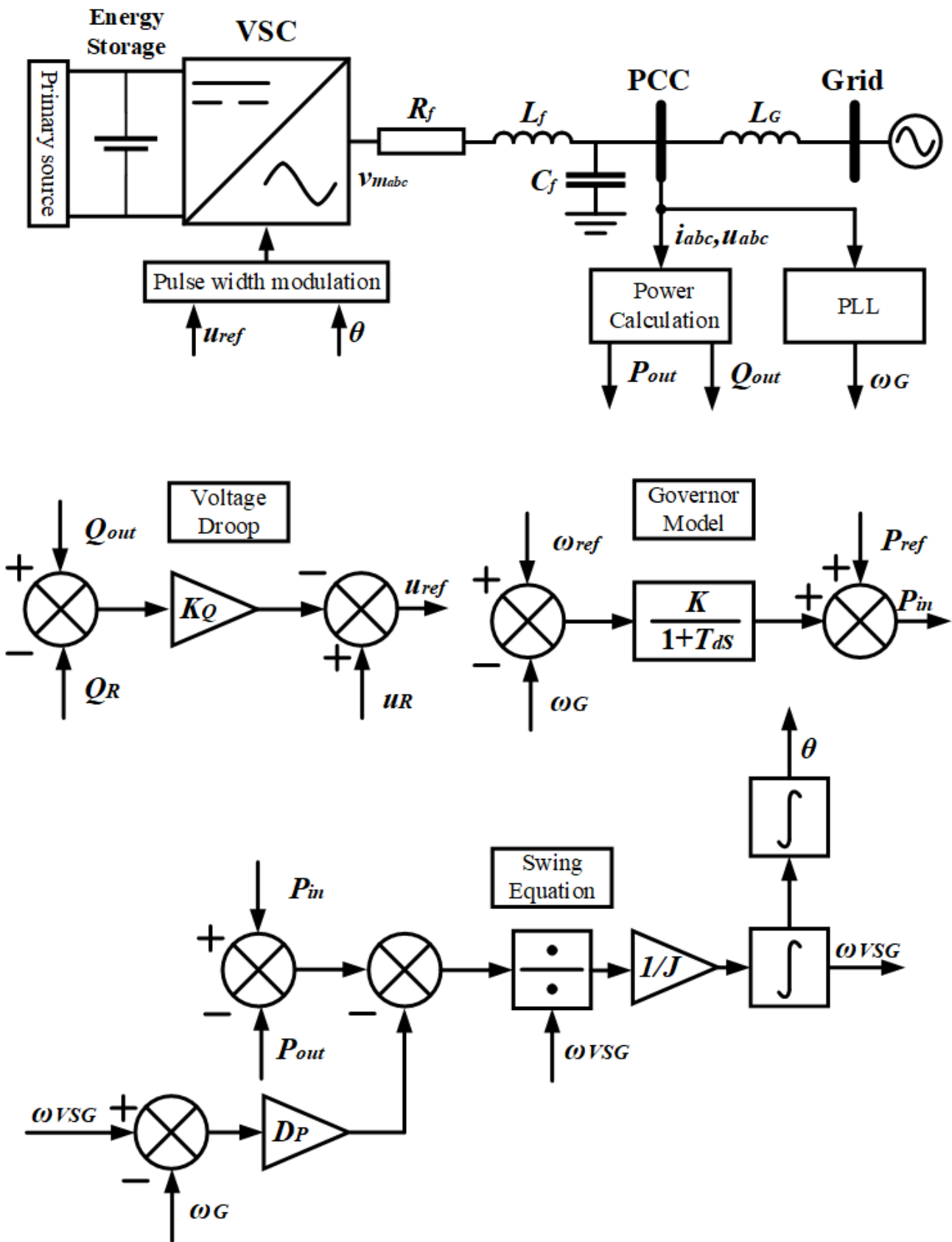


Figure 18 - ISE Labs topology structure and block diagram

VSYNC

The main difference between the VSYNC topology and described above is that one of the inputs is the battery state of charge. The change in Δsoc of this charge is one of the components of the output power equation. In this way, the inertia of the rotating masses of traditional synchronous machines is simulated [17].

Structurally, VSYNC is focused on simulating the inertial response of a synchronous machine [16]. The electromagnetic processes in the synchronous machine are not considered within this topology, only the AVR operates when voltage change occurs.

The inputs, in addition to the state of charge of the battery, are the phase voltages and currents in the CCP, as well as the phase of the grid's voltage, the increment of its frequency and its rate of change. The input voltages are converted from the three-phase coordinate system to the dq system via the Park transformation, and then the values obtained are fed to the reactive power droop block input, forming the reactive power setpoint.

The active power setpoint is generated based on the battery charge state and the PLL measurement results. The resulting power setpoints are used to calculate reference currents in dq coordinates. These currents are then converted to a three-phase coordinate system and fed to the controller input, which calculates the reference voltage based on the reference currents and measured phase currents and voltages in the CCP, which is the control signal for the pulse-width modulation unit.

There are a number of significant disadvantages to this topology. For example, the application of the PLL is required not only at the stage of initial synchronization with the grid frequency, as in all of the above topologies, but throughout the operation of the algorithm [16]. One of the input signals of the active power set point generation block is the system frequency derivative, which can lead to additional signal distortions in the topology.

It's also worth mentioning that topology is focused on frequency change - both its deviation and speed of change are considered, while AVR system reacts only to voltage increment.

Structure and block diagrams of this topology are shown on Figure 19 [16, 17, 21].

The considered topologies, being the most widespread, have a number of disadvantages. Among them are the lack of precise description of processes in the synchronous machine (VSE, ISE labs topologies), application of torques as inputs in swing equation (VISMA, Synchronverter and ISE Labs topologies) or application of frequency derivative for this purpose (VSYNC topology) and implementation of PLL in all the considered topologies.

These disadvantages are avoided in the structure of proposed PC control algorithm – VSG-C (current-controlled VSG). A detailed description of this topology is given below.

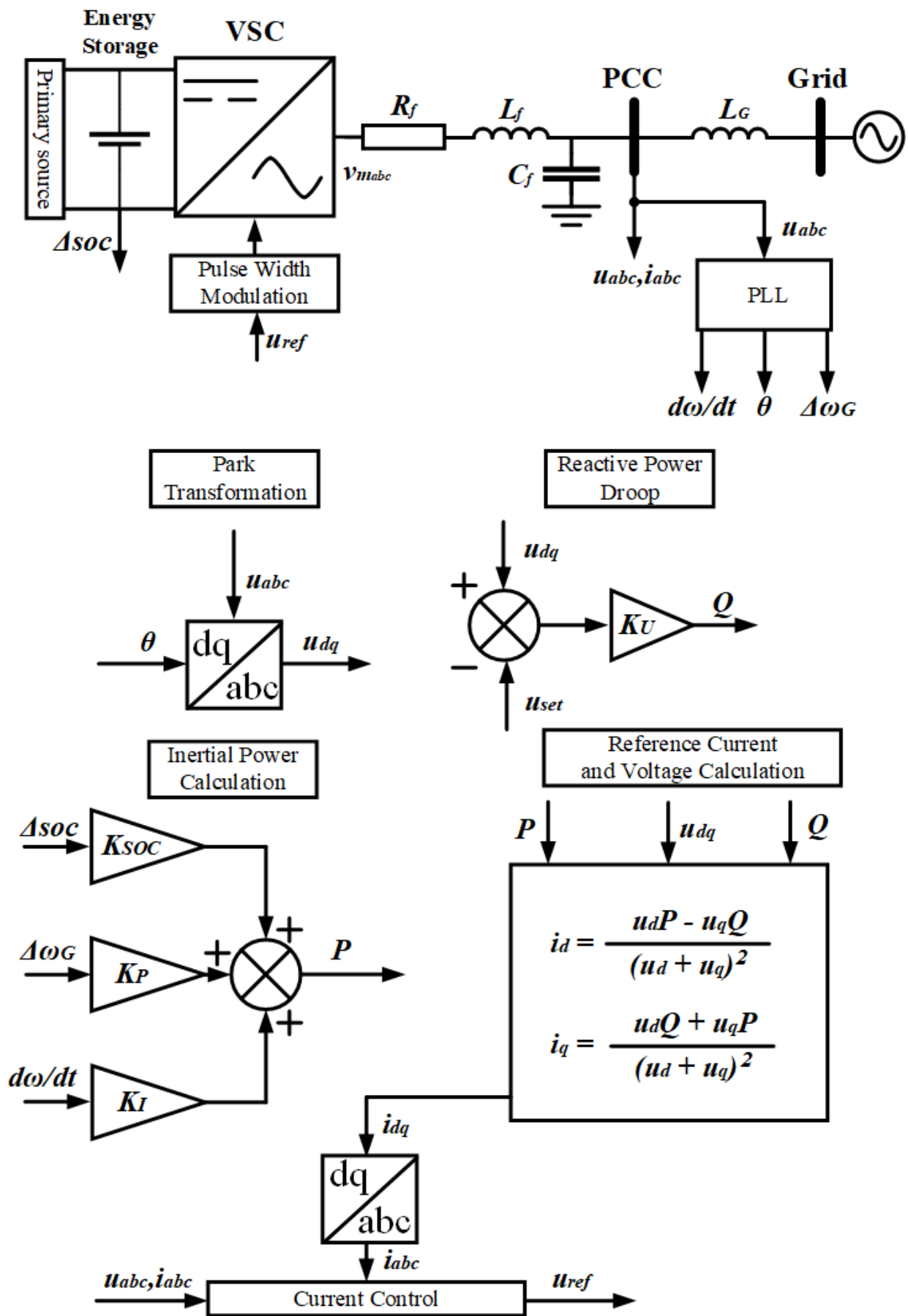


Figure 19 - Structure and block diagram of the VSYNC topology

2.2. VSG – C topology

The VSG-C structure and block diagram is shown in Figure 20.

The inputs of the topology are the three-phase voltages in the CCP as well as the output currents of the VSG fed to the input of the filtering device. All calculations are performed in the synchronous dq coordinate system, so the input quantities go through the Park transformation.

The electromechanical part of this topology is represented by the swing equation implemented on the basis of magnitudes rather instead of moments, as in the VISMA and Synchronverter topologies, which increases its reliability since there is no division by frequency and, therefore, the probability of solution instability is reduced. Frequency controller is based on frequency droop, similar to Synchronverter and ISE Labs topologies. In this topology, similar to VISMA topologies, a damping circuit is performed, but in a more complex implementation: the damping factor is excluded, virtual damping circuit is simulated.

The inputs of the electromechanical part are the calculated frequency ω_{VSG} and the output power P_{VSG} of the VSG. The frequency is compared with the setpoint ω_{set} and the mismatch signal multiplied by the frequency droop factor K_ω is fed to the motion equation input, where it is compared with the output active power setpoint $P_{set,VSG}$ and the instantaneous output power P_{VSG} . On the basis of the power mismatch, considering the VSG inertia constant, the frequency ω_{VSG} and the phase θ_{VSG} of the output voltage are calculated. All calculations are performed in relative units.

The electromagnetic processes of a synchronous machine reproduced by this topology correspond to a simplified equivalent circuit of a conventional synchronous machine. They are implemented through virtual stator winding resistance R_V and inductance L_V , virtual transformation and rotation EMFs. The electromagnetic processes of a synchronous machine reproduced by this topology correspond to a simplified equivalent circuit of a conventional synchronous machine. They are

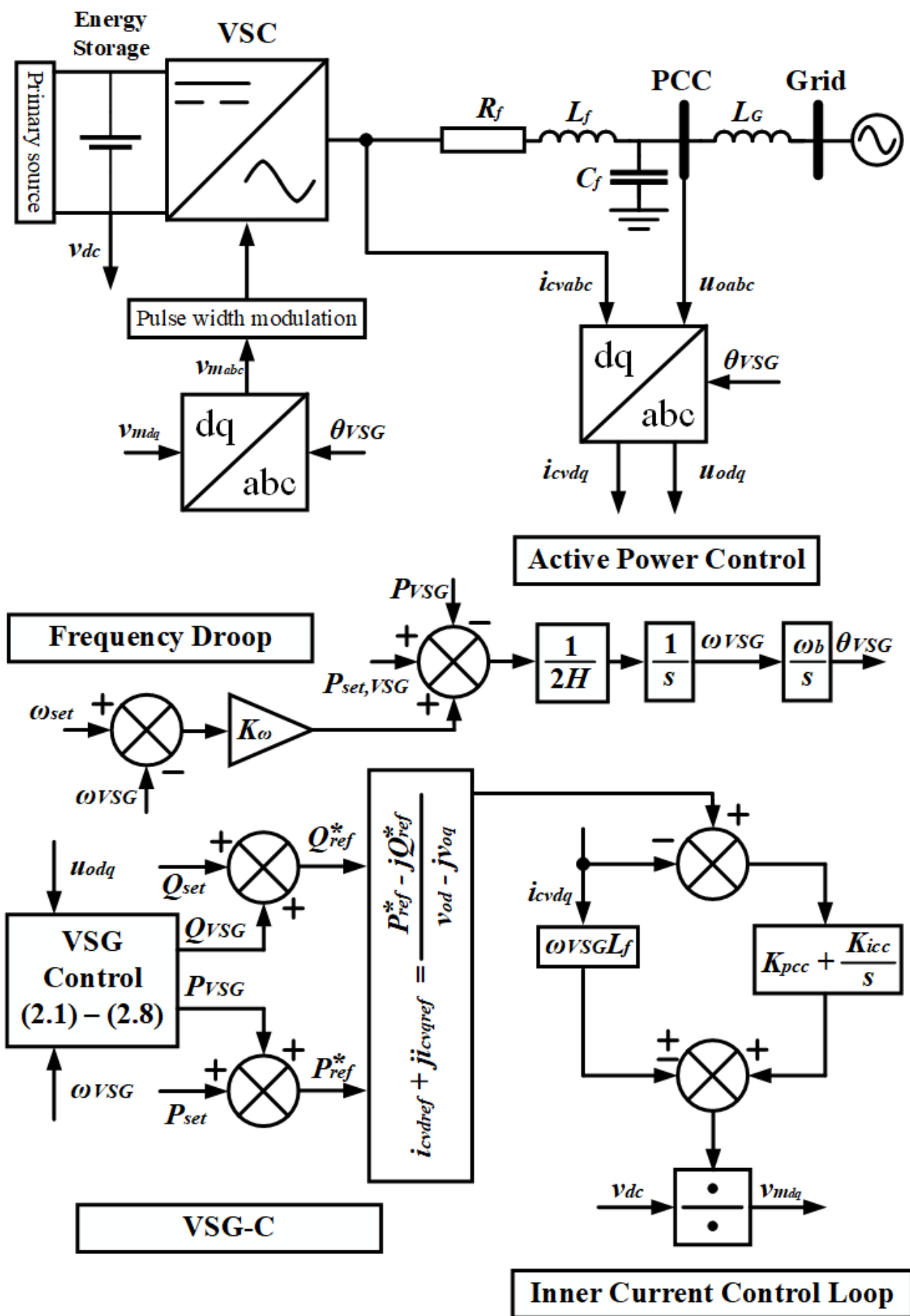


Figure 20 - Structure and block diagram of the VSG-C topology

implemented through virtual stator winding resistance R_V and inductance L_V , virtual transformation and rotation EMFs. By means of an ideal virtual excitation winding along the d-axis to reproduce the necessary ψ_{fd} current coincidence, the exciter operation is considered. Also, as mentioned earlier, the topology is simplified by excluding the stray inductance to represent the damping circuit along the q-axis.

The equivalent circuit of the electrical part of the VSG topology VSG-C is shown in Figure 21.

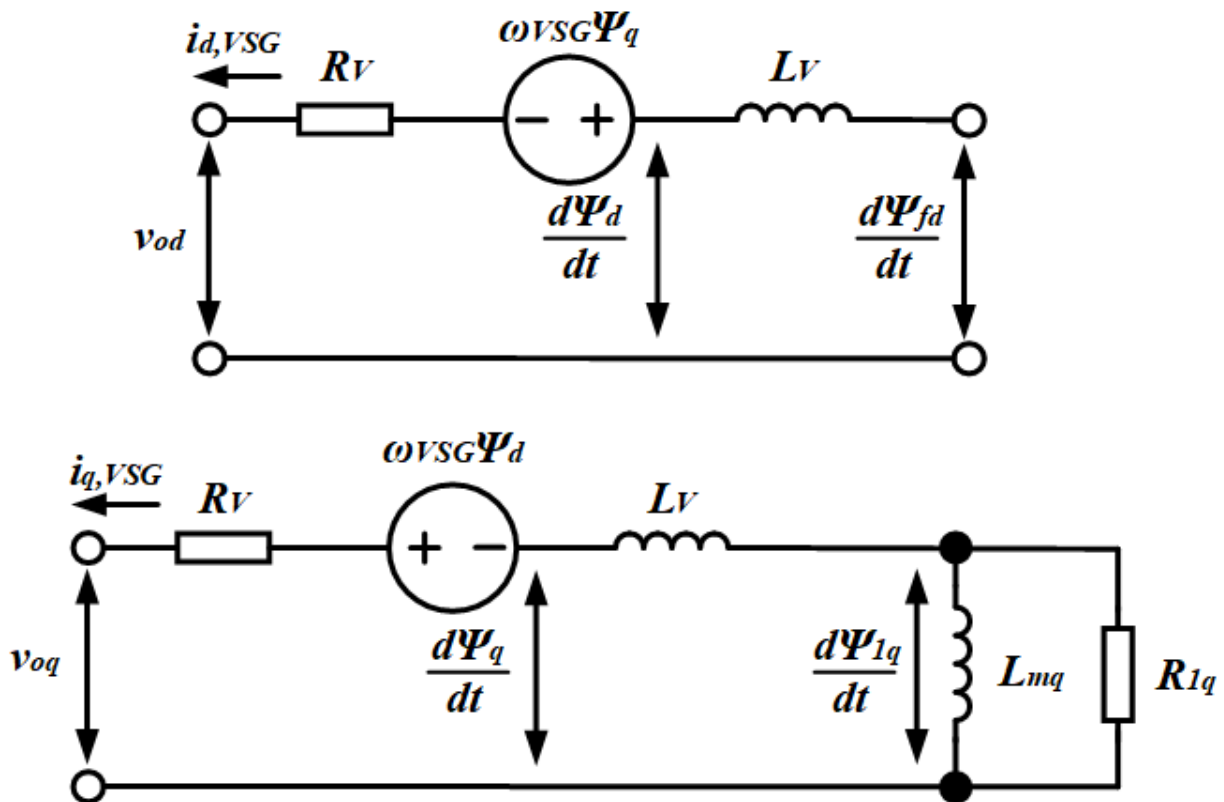


Figure 21 - Electrical substitution diagram for WASH topology VSG-C

Equations describing the electrical part are given in expressions (2.1.) to (2.8.).

$$\left\{ \begin{array}{l} \frac{d\psi_d}{dt} = \omega_b \cdot (v_{od} + R_V \cdot i_{d,VSG} + \omega_{VSG} \cdot \psi_q) \quad (2.1.) \\ \frac{d\psi_q}{dt} = \omega_b \cdot (v_{oq} + R_V \cdot i_{q,VSG} - \omega_{VSG} \cdot \psi_d) \quad (2.2.) \\ \frac{d\psi_{1q}}{dt} = \omega_b \cdot \left(-R_{1q} \cdot I_{q,VSG} - \frac{R_{1q}}{L_{1q}} \cdot \psi_{1q} \right) \quad (2.3.) \\ \frac{d\psi_{fd}}{dt} = K_v \cdot \left(\frac{Q_{set,VSG} - Q_{VSG}}{V_o} \right) \quad (2.4.) \\ i_{d,VSG} = \frac{\psi_{fd} - \psi_d}{L_V} \quad (2.5.) \\ i_{q,VSG} = \frac{\psi_{1q} - \psi_q}{L_V} \quad (2.6.) \\ P_{VSG} = v_{od} \cdot i_{d,VSG} + v_{oq} \cdot i_{q,VSG} \quad (2.7.) \\ Q_{VSG} = v_{oq} \cdot i_{d,VSG} - v_{od} \cdot i_{q,VSG} \quad (2.8.) \end{array} \right.$$

In this formulas ψ_d and ψ_q – magnetic fluxes of virtual stator winding through d and q axes, ψ_{1q} – magnetic flux of virtual damper winding through q axe, R_{1q} и L_{1q} – active resistance and inductance of virtual exciter, $Q_{set,VSG}$ – setpoint of VSG's reactive power, Q_{VSG} – calculated value of VSG's reactive power output, K_v – gain of reactive power control loop, v_{odq} – VSG voltage in dq axes.

One of the features of the proposed VSG-C topology is the parallel operation of the reference loops. One of them is responsible for generating the active P_{set} and reactive Q_{set} power settings. The second loop generates the output active P_{VSG} and reactive Q_{VSG} powers of the VSG on the basis of the results of the calculation of the electromagnetic processes model in the synchronous machine. The resulting setting values are added to the calculated powers of the VSG, resulting in the reference values of active P_{ref}^* and reactive Q_{ref}^* powers. Based on the reference powers, the current reference values i_{cvdref} and i_{cvqref} are generated for the internal current control loop by expression (2.9.):

$$i_{cvdref} + j i_{cvqref} = \frac{P_{ref}^* - j Q_{ref}^*}{v_{od} - j v_{oq}} \quad (2.9.)$$

In this formula v_{od} and v_{oq} – voltages of CCP in dq axes.

It is important to note that this topology assumes zero load, i.e. $P_{set} = Q_{set} = 0$. Also, another feature is the absence of PLL.

Compared to the VSG topologies described above, the proposed VSG-C topology has several advantages:

1. Excluding of PLL increases reliability and stability of operation
2. The synchronous machine model describes its processes in sufficient detail. At the same time, there is no unnecessary detail that can slow down the response and reduce the robustness of the solution
3. The use of powers as input quantities to the electro-mechanical part of the VSG. The removal of the division by frequency operation that is necessary to describe the equation of motion through torques increases the reliability of the topology

It is worth noting that the simulation of the damping winding by a separate circuit and the corresponding differential equation reduces the reliability of the model, increasing the probability of instability of the numerical solution.

In the following sections, the properties and response of the VSG-C topology at small-signal and within a two-machine system will be investigated.

3. Investigation of VSG-C topology

This section investigates the properties and response of the proposed MBIII-C topology. The response when participating in network mode control will be considered.

To simulate the response of the topology during its participation in the regulation of grid mode will be used small-signal technique. To apply it a linearized model of the system is required. Thus, a complete mathematical model of the system under study in the state space, including, as follows from Figure 20, a power converter controlled on the basis of the VSG-C, a filtering device consisting of an active resistance R_f , inductance L_f and capacitance C_f , and an electrical system equivalent to a voltage source V_G and a communication line with an active resistance R_G and inductance L_G based on Thevenin's theorem, is required in advance.

This part of the work is carried out using the Matlab/Simulink software package.

The linearized response is verified in the PSCAD software package. This does not require a state-space model, blocks from its internal libraries are used, which provide the basis for a final model which consists structurally of the same basic parts as the state-space model.

Thus, this section is structured as follows. Subsection 3.1 is devoted to the compilation and linearization of the system under consideration in the state space. Subsection 3.2 investigates in detail the response of the linearized model. In subsection 3.3, the response of a detailed nonlinear topology model of the VSG-C assembled in the PSCAD software package is investigated and compared to the response of the linearized model.

3.1. Linearized state-space model of VSG-C

The system is described through 14 state variables and system of 14 differential equations. To combine this system it is necessary to consider equations (2.1) – (2.9) from Section 2, equations (3.1) – (3.4) which describe the process of forming of voltage references for inner current control loop, and (3.5) – (3.10) which describe grid and RLC-filter.

$$\left\{ \begin{array}{l} v_{cvdref} = k_{PCC} \cdot (i_{cvdref} - i_{cvd}) + k_{iCC} \cdot \xi_d - L_f \cdot \omega_{VSG} \cdot i_{cvq} \quad (3.1) \\ v_{cvqref} = k_{PCC} \cdot (i_{cvqref} - i_{cvq}) + k_{iCC} \cdot \xi_q + L_f \cdot \omega_{VSG} \cdot i_{cvd} \quad (3.2) \\ \frac{d\xi_d}{dt} = i_{cvdref} - i_{cvd} \quad (3.3) \\ \frac{d\xi_q}{dt} = i_{cvqref} - i_{cvq} \quad (3.4) \end{array} \right.$$

$$\left\{ \begin{array}{l} \frac{di_{cvd}}{dt} = \frac{\omega_b}{L_f} \cdot v_{cvdref} - \frac{\omega_b}{L_f} \cdot v_{od} - \frac{\omega_b \cdot R_f}{L_f} \cdot i_{cvd} + \omega_b \cdot \omega_G \cdot i_{cvq} \quad (3.5) \end{array} \right.$$

$$\left\{ \begin{array}{l} \frac{di_{cvq}}{dt} = \frac{\omega_b}{L_f} \cdot v_{cvqref} - \frac{\omega_b}{L_f} \cdot v_{oq} - \frac{\omega_b \cdot R_f}{L_f} \cdot i_{cvq} - \omega_b \cdot \omega_G \cdot i_{cvd} \quad (3.6) \end{array} \right.$$

$$\left\{ \begin{array}{l} \frac{dv_{od}}{dt} = \frac{\omega_b}{C_f} \cdot i_{cvd} - \frac{\omega_b}{C_f} \cdot i_{od} + \omega_b \cdot \omega_G \cdot v_{oq} \quad (3.7) \end{array} \right.$$

$$\left\{ \begin{array}{l} \frac{dv_{oq}}{dt} = \frac{\omega_b}{C_f} \cdot i_{cvq} - \frac{\omega_b}{C_f} \cdot i_{oq} - \omega_b \cdot \omega_G \cdot v_{od} \quad (3.8) \end{array} \right.$$

$$\left\{ \begin{array}{l} \frac{di_{od}}{dt} = \frac{\omega_b}{L_G} \cdot v_{od} - \frac{\omega_b}{L_G} \cdot V_G \cdot \sin \theta_{VSG} - \frac{\omega_b \cdot R_G}{L_G} \cdot i_{od} + \omega_b \cdot \omega_G \cdot i_{oq} \quad (3.9) \end{array} \right.$$

$$\left\{ \begin{array}{l} \frac{di_{oq}}{dt} = \frac{\omega_b}{L_G} \cdot v_{oq} - \frac{\omega_b}{L_G} \cdot V_G \cdot \cos \theta_{VSG} - \frac{\omega_b \cdot R_G}{L_G} \cdot i_{oq} - \omega_b \cdot \omega_G \cdot i_{od} \quad (3.10) \end{array} \right.$$

Thus it is possible to construct mathematical model consisting equations (3.11) – (3.24) which are listed below.

$$\frac{dv_{od}}{dt} = \omega_b \omega_G v_{oq} + \frac{\omega_b}{C_f} i_{cvd} - \frac{\omega_b}{C_f} i_{od} \quad (3.11)$$

$$\frac{dv_{oq}}{dt} = -\omega_b \omega_G v_{od} + \frac{\omega_b}{C_f} i_{cvq} - \frac{\omega_b}{C_f} i_{oq} \quad (3.12)$$

$$\frac{di_{cvd}}{dt} = - \quad (3.13)$$

$$\frac{di_{cvq}}{dt} = - \quad (3.14)$$

$$\frac{d\xi_d}{dt} = - \frac{v_{od}^2 \psi_d - v_{od}^2 \psi_{fd} + v_{oq}^2 \psi_d - v_{oq}^2 \psi_{fd} - L_d Q_{ref} v_{oq} + \dots}{L_d (v_{od}^2 + v_{oq}^2)} + \dots$$

$$\frac{+L_d i_{cvq} v_{od}^2 + L_d i_{cvd} v_{oq}^2 - L_d P_{ref} v_{od}}{L_d (v_{od}^2 + v_{oq}^2)} \quad (3.15)$$

$$\frac{d\xi_q}{dt} = - \frac{v_{od}^2 \psi_q + v_{oq}^2 \psi_q - v_{od}^2 \psi_{1q} - v_{oq}^2 \psi_{1q} - L_q Q_{ref} v_{od} + \dots}{L_d (v_{od}^2 + v_{oq}^2)} + \dots$$

$$\frac{+L_d i_{cvq} v_{od}^2 + L_d i_{cvd} v_{oq}^2 - L_d P_{ref} v_{od}}{L_d (v_{od}^2 + v_{oq}^2)} \quad (3.16)$$

$$\frac{di_{od}}{dt} = \frac{\omega_b}{L_G} v_{od} - \frac{\omega_b R_G}{L_G} i_{od} + \omega_b \omega_G i_{oq} - \frac{\omega_b}{L_G} V_G \cos \theta_{VSG} \quad (3.17)$$

$$\frac{di_{oq}}{dt} = \frac{\omega_b}{L_G} v_{oq} - \frac{\omega_b R_G}{L_G} i_{oq} - \omega_b \omega_G i_{od} + \frac{\omega_b}{L_G} V_G \sin \theta_{VSG} \quad (3.18)$$

$$\frac{d\psi_d}{dt} = \omega_b v_{od} + \frac{\omega_b R_V}{L_d} \psi_{fd} - \frac{\omega_b R_V}{L_d} \psi_d + \omega_b \cdot (\omega_{VSG} + \omega_G) \cdot \psi_q \quad (3.19)$$

$$\frac{d\psi_q}{dt} = \omega_b v_{oq} + \frac{\omega_b R_V}{L_q} \psi_{1q} - \frac{\omega_b R_V}{L_d} \psi_q - \omega_b \cdot (\omega_{VSG} + \omega_G) \cdot \psi_d \quad (3.20)$$

$$\frac{d\psi_{1q}}{dt} = -\omega_b R_{1q} \cdot \left(\frac{1}{L_{1q}} + \frac{1}{L_q} \right) \cdot \psi_{1q} + \frac{\omega_b R_{1q}}{L_q} \psi_q \quad (3.21)$$

$$\frac{d\psi_{fd}}{dt} = \frac{k_{fd} (L_q v_{oq} \psi_d - L_d v_{od} \psi_q - L_q v_{oq} \psi_{fd} + L_d v_{od} \psi_{1q} + L_d L_q Q_{set})}{L_d L_q \sqrt{v_{od}^2 + v_{oq}^2}}$$

$$\frac{d\theta_{VSG}}{dt} = \omega_b \omega_{VSG} \quad (3.23)$$

$$\frac{d\omega_{VSG}}{dt} = -\frac{1}{T_{exc}} \cdot \left(\frac{\psi_{fd} - \psi_d}{L_d} \right) v_{od} - \frac{1}{T_{exc}} \cdot \left(\frac{\psi_{1q} - \psi_q}{L_q} \right) v_{oq} + \frac{1}{T_{exc}} \cdot P_{set,VSG} \quad (3.24)$$

In general terms, the resulting state-space model can be represented as equation (3.25):

$$\dot{X} = A \cdot X + B \cdot U \quad (3.25)$$

In this formula \dot{X} – array vector of state variables derivatives, X – array vector of state variables, U – array vector of inputs, A – state matrix, B – matrix of inputs coefficients.

Linearizing this model means reducing it to the form (3.26):

$$\Delta\dot{X} = A(X_0) \cdot \Delta X + B(X_0) \cdot \Delta U \quad (3.26)$$

In this formula $\Delta\dot{X}$ – array vector of linearized state variables derivatives, ΔX – array vector of linearized state variables, ΔU – array vector of linearized inputs, $A(X_0)$ – transformed as a result of linearization state matrix, $B(X_0)$ – transformed as a result of linearization matrix of inputs coefficients.

A detailed representation of each element of equation (3.26) is given in expressions (3.27) to (3.59):

$$A(X_0) = \begin{bmatrix} AA_1^T \\ AA_2^T \\ AA_3^T \\ AA_4^T \\ AA_5^T \\ AA_6^T \\ AA_7^T \\ AA_8^T \\ AA_9^T \\ AA_{10}^T \\ AA_{11}^T \\ AA_{12}^T \\ AA_{13}^T \\ AA_{14}^T \end{bmatrix} \quad (3.27) \quad B(X_0) = \begin{bmatrix} BB_1^T \\ BB_2^T \\ BB_3^T \\ BB_4^T \\ BB_5^T \\ BB_6^T \\ BB_7^T \\ BB_8^T \\ BB_9^T \\ BB_{10}^T \\ BB_{11}^T \\ BB_{12}^T \\ BB_{13}^T \\ BB_{14}^T \end{bmatrix} \quad (3.28) \quad \Delta U = \begin{bmatrix} \Delta P_{set} \\ \Delta Q_{set} \\ \Delta P_{set,VSG} \\ \Delta Q_{set,VSG} \\ \Delta V_G \\ \Delta \omega_G \end{bmatrix} \quad (3.29)$$

$$\Delta X = \begin{bmatrix} \Delta v_{od} \\ \Delta v_{oq} \\ \Delta i_{cvd} \\ \Delta i_{cvq} \\ \Delta \xi_d \\ \Delta \xi_q \\ \Delta i_{od} \\ \Delta i_{oq} \\ \Delta \psi_d \\ \Delta \psi_q \\ \Delta \psi_{1q} \\ \Delta \psi_{fd} \\ \Delta \theta_{VSG} \\ \Delta \omega_{VSG} \end{bmatrix} \quad (3.30)$$

$$\Delta \dot{X} = \begin{bmatrix} \frac{d\Delta v_{od}}{dt} \\ \frac{d\Delta v_{oq}}{dt} \\ \frac{d\Delta i_{cvd}}{dt} \\ \frac{d\Delta i_{cvq}}{dt} \\ \frac{d\Delta \xi_d}{dt} \\ \frac{d\Delta \xi_q}{dt} \\ \frac{d\Delta i_{od}}{dt} \\ \frac{d\Delta i_{oq}}{dt} \\ \frac{d\Delta \psi_d}{dt} \\ \frac{d\Delta \psi_q}{dt} \\ \frac{d\Delta \psi_{1q}}{dt} \\ \frac{d\Delta \psi_{fd}}{dt} \\ \frac{d\Delta \theta_{VSG}}{dt} \\ \frac{d\Delta \omega_{VSG}}{dt} \end{bmatrix} \quad (3.31)$$

$$BB_1 = \begin{bmatrix} 0 \\ 0 \\ 0 \\ 0 \\ 0 \\ \omega_b v_{oq0} \end{bmatrix} \quad (3.32)$$

$$BB_2 = \begin{bmatrix} 0 \\ 0 \\ 0 \\ 0 \\ 0 \\ -\omega_b v_{od0} \end{bmatrix} \quad (3.33)$$

$$BB_3 = \begin{bmatrix} \frac{\omega_b K_{PCC} v_{od0}}{L_f(v_{od0}^2 + v_{od0}^2)} \\ \frac{\omega_b K_{PCC} v_{oq0}}{L_f(v_{od0}^2 + v_{od0}^2)} \\ 0 \\ 0 \\ 0 \\ 0 \end{bmatrix} \quad (3.34) \quad BB_4 = \begin{bmatrix} \frac{\omega_b K_{PCC} v_{oq0}}{L_f(v_{od0}^2 + v_{od0}^2)} \\ -\frac{\omega_b K_{PCC} v_{od0}}{L_f(v_{od0}^2 + v_{od0}^2)} \\ 0 \\ 0 \\ 0 \\ 0 \end{bmatrix} \quad (3.35)$$

$$BB_5 = \begin{bmatrix} \frac{v_{od0}}{v_{od0}^2 + v_{oq0}^2} \\ \frac{v_{oq0}}{v_{od0}^2 + v_{oq0}^2} \\ 0 \\ 0 \\ 0 \\ 0 \end{bmatrix} \quad (3.36) \quad BB_6 = \begin{bmatrix} \frac{v_{oq0}}{v_{od0}^2 + v_{oq0}^2} \\ -\frac{v_{od0}}{v_{od0}^2 + v_{oq0}^2} \\ 0 \\ 0 \\ 0 \\ 0 \end{bmatrix} \quad (3.37)$$

$$BB_7 = \begin{bmatrix} 0 \\ 0 \\ 0 \\ 0 \\ -\frac{\omega_b \sin \theta_{VSG0}}{L_G} \\ \omega_b i_{oq0} \end{bmatrix} \quad (3.38) \quad BB_8 = \begin{bmatrix} 0 \\ 0 \\ 0 \\ 0 \\ -\frac{\omega_b \cos \theta_{VSG0}}{L_G} \\ -\omega_b i_{od0} \end{bmatrix} \quad (3.39)$$

$$BB_9 = \begin{bmatrix} 0 \\ 0 \\ 0 \\ 0 \\ 0 \\ \omega_b \psi_{q0} \end{bmatrix} \quad (3.40) \quad BB_{10} = \begin{bmatrix} 0 \\ 0 \\ 0 \\ 0 \\ 0 \\ -\omega_b \psi_{d0} \end{bmatrix} \quad (3.41) \quad BB_{11} = \begin{bmatrix} 0 \\ 0 \\ 0 \\ 0 \\ 0 \\ 0 \end{bmatrix} \quad (3.42)$$

$$BB_{12} = \begin{bmatrix} 0 \\ 0 \\ 0 \\ 1 \\ \frac{T_{exc} V_{G0}}{T_{exc} L_V^2 V_{G0}^2} \\ -\frac{L_V v_{oq0} \psi_{d0} - L_V v_{od0} \psi_{q0} - L_V v_{oq0} \psi_{fd0} + L_V v_{od0} \psi_{1q0} + L_V^2 Q_{set, VSG0}}{T_{exc} L_V^2 V_{G0}^2} \\ 0 \end{bmatrix} \quad (3.43)$$

$$BB_{13} = \begin{bmatrix} 0 \\ 0 \\ 0 \\ 0 \\ 0 \\ 0 \end{bmatrix} \quad (3.44) \quad BB_{14} = \begin{bmatrix} 0 \\ 0 \\ 1 \\ 0 \\ 0 \\ 0 \end{bmatrix} \quad (3.45)$$

$$AA_1 = \begin{bmatrix} 0 \\ \omega_b \omega_{G0} \\ \frac{\omega_b}{C_f} \\ 0 \\ 0 \\ 0 \\ -\frac{\omega_b}{C_f} \\ 0 \\ 0 \\ 0 \\ 0 \\ 0 \\ 0 \\ 0 \\ 0 \end{bmatrix} \quad (3.46) \quad AA_2 = \begin{bmatrix} -\omega_b \omega_{G0} \\ 0 \\ 0 \\ \frac{\omega_b}{C_f} \\ 0 \\ 0 \\ 0 \\ 0 \\ -\frac{\omega_b}{C_f} \\ 0 \\ 0 \\ 0 \\ 0 \\ 0 \\ 0 \end{bmatrix} \quad (3.47)$$

$$AA_3 = \begin{bmatrix} \frac{\omega_b(v_{od0}^4 + 2v_{od0}^2 v_{oq0}^2 + P_{set0} K_{PCC} v_{od0}^2 + 2Q_{set0} K_{PCC} v_{od0} v_{oq0} + v_{oq0}^4 - P_{set0} K_{PCC} v_{oq0}^2)}{L_f(v_{od0}^2 + v_{oq0}^2)} \\ -\frac{\omega_b K_{PCC} (2P_{set0} v_{od0} v_{oq0} - Q_{set0} v_{od0}^2 + Q_{set0} v_{oq0}^2)}{L_f(v_{od0}^2 + v_{oq0}^2)^2} \\ -\frac{\omega_b (K_{PCC} + R_f)}{L_f} \\ -\omega_b \omega_{VSG0} \\ \frac{\omega_b K_{icc}}{L_f} \\ 0 \\ 0 \\ 0 \\ -\frac{\omega_b K_{PCC}}{L_V L_f} \\ 0 \\ 0 \\ -\frac{\omega_b K_{PCC}}{L_V L_f} \\ 0 \\ 0 \end{bmatrix} \quad (3.48)$$

$$AA_4 = \begin{bmatrix} -\frac{\omega_b K_{PCC} (2P_{set0} v_{od0} v_{oq0} - Q_{set0} v_{od0}^2 + Q_{set0} v_{oq0}^2)}{L_f (v_{od0}^2 + v_{oq0}^2)^2} \\ -\frac{\omega_b (v_{od0}^4 + 2v_{od0}^2 v_{oq0}^2 - P_{set0} K_{PCC} v_{od0}^2 - 2Q_{set0} K_{PCC} v_{od0} v_{oq0} + v_{oq0}^4 + P_{set0} K_{PCC} v_{oq0}^2)}{L_f (v_{od0}^2 + v_{oq0}^2)} \\ \frac{\omega_b \omega_{VSG0}}{\omega_b (K_{PCC} + R_f)} \\ -\frac{L_f}{0} \\ \frac{\omega_b K_{icc}}{L_f} \\ 0 \\ 0 \\ 0 \\ \frac{\omega_b K_{PCC}}{L_V L_f} \\ \frac{\omega_b K_{PCC}}{L_V L_f} \\ 0 \\ 0 \\ \omega_b i_{od0} \end{bmatrix} \quad (3.49)$$

$$AA_5 = \begin{bmatrix} -\frac{P_{set0} v_{od0}^2 + 2Q_{set0} v_{od0} v_{oq0} - P_{set0} v_{oq0}^2}{(v_{od0}^2 + v_{oq0}^2)^2} \\ -\frac{2P_{set0} v_{od0} v_{oq0} - Q_{set0} v_{od0}^2 + Q_{set0} v_{oq0}^2}{(v_{od0}^2 + v_{oq0}^2)^2} \\ -1 \\ 0 \\ 0 \\ 0 \\ 0 \\ 0 \\ -\frac{1}{L_V} \\ 0 \\ 0 \\ \frac{1}{L_V} \\ 0 \\ 0 \end{bmatrix} \quad (3.50)$$

$$AA_6 = \begin{bmatrix} \frac{2P_{set0}v_{od0}v_{oq0} - Q_{set0}v_{od0}^2 + Q_{set0}v_{oq0}^2}{(v_{od0}^2 + v_{oq0}^2)^2} \\ \frac{P_{set0}v_{od0}^2 + 2Q_{set0}v_{od0}v_{oq0} - P_{set0}v_{oq0}^2}{(v_{od0}^2 + v_{oq0}^2)^2} \\ 0 \\ -1 \\ 0 \\ 0 \\ 0 \\ 0 \\ 0 \\ \frac{1}{L_V} \\ \frac{1}{L_V} \\ 0 \\ 0 \\ 0 \end{bmatrix} \quad (3.51)$$

$$AA_7 = \begin{bmatrix} \frac{\omega_b}{L_G} \\ 0 \\ 0 \\ 0 \\ 0 \\ 0 \\ -\frac{\omega_b R_G}{L_G} \\ \omega_b \omega_{G0} \\ 0 \\ 0 \\ 0 \\ 0 \\ 0 \\ -\frac{\omega_b V_{G0} \cos \theta_{VSG0}}{L_G} \\ 0 \end{bmatrix} \quad (3.52)$$

$$AA_8 = \begin{bmatrix} 0 \\ \frac{\omega_b}{L_G} \\ 0 \\ 0 \\ 0 \\ 0 \\ -\omega_b \omega_{G0} \\ -\frac{\omega_b R_G}{L_G} \\ 0 \\ 0 \\ 0 \\ 0 \\ 0 \\ \frac{\omega_b V_{G0} \sin \theta_{VSG0}}{L_G} \\ 0 \end{bmatrix} \quad (3.53)$$

$$AA_9 = \begin{bmatrix} \omega_b \\ 0 \\ 0 \\ 0 \\ 0 \\ 0 \\ 0 \\ 0 \\ -\frac{\omega_b R_V}{L_V} \\ \omega_b(\omega_{VSG0} + \omega_{G0}) \\ 0 \\ \frac{\omega_b R_V}{L_V} \\ 0 \\ \omega_b \psi_{q0} \end{bmatrix} \quad (3.54)$$

$$AA_{10} = \begin{bmatrix} 0 \\ \omega_b \\ 0 \\ 0 \\ 0 \\ 0 \\ 0 \\ 0 \\ -\omega_b(\omega_{VSG0} + \omega_{G0}) \\ \frac{\omega_b R_V}{L_V} \\ \frac{\omega_b R_V}{L_V} \\ 0 \\ 0 \\ -\omega_b \psi_{d0} \end{bmatrix} \quad (3.55)$$

$$AA_{11} = \begin{bmatrix} 0 \\ 0 \\ 0 \\ 0 \\ 0 \\ 0 \\ 0 \\ 0 \\ 0 \\ \frac{\omega_b R_{1q}}{L_V} \\ -\frac{\omega_b R_{1q}(L_V + L_{1q})}{L_V L_{1q}} \\ 0 \\ 0 \\ 0 \end{bmatrix} \quad (3.56)$$

$$AA_{12} = \begin{bmatrix} \frac{\psi_{1q0} - \psi_{q0}}{T_{exc} L_V V_{G0}} \\ \frac{\psi_{d0} - \psi_{fd0}}{T_{exc} L_V V_{G0}} \\ 0 \\ 0 \\ 0 \\ 0 \\ 0 \\ 0 \\ 0 \\ \frac{v_{oq0}}{T_{exc} L_V V_{G0}} \\ \frac{v_{od0}}{T_{exc} L_V V_{G0}} \\ \frac{v_{oq0}}{T_{exc} L_V V_{G0}} \\ 0 \\ 0 \end{bmatrix} \quad (3.57)$$

$$AA_{13} = \begin{bmatrix} 0 \\ 0 \\ 0 \\ 0 \\ 0 \\ 0 \\ 0 \\ 0 \\ 0 \\ 0 \\ 0 \\ 0 \\ 0 \\ 0 \\ \omega_b \end{bmatrix} \quad (3.58)$$

$$AA_{14} = \begin{bmatrix} \frac{\psi_{d0} - \psi_{fd0}}{2HL_V} \\ \frac{\psi_{q0} - \psi_{1q0}}{2HL_V} \\ 0 \\ 0 \\ 0 \\ 0 \\ 0 \\ 0 \\ \frac{v_{od0}}{2HL_V} \\ \frac{v_{oq0}}{2HL_V} \\ -\frac{v_{oq0}}{2HL_V} \\ \frac{v_{od0}}{2HL_V} \\ 0 \\ 0 \end{bmatrix} \quad (3.59)$$

3.2. Investigation of linearized VSG-C response

In this section participation of VSG in regulation process is considered by changing the value of P_{set} from 0 to 0.7 p.u at the 5 s. By this the response of regulation system is considered: when frequency decreases it is necessary to increase the value of generated power due to equalize ROCOF to zero at first and then to return the value of frequency to the rated one.

Meanwhile the voltage deviation occurs too and it is possible to notice the process of voltage governing.

Curves of changing of voltage, reactive power, active power and frequency deviation are represented in figures 22 – 25.

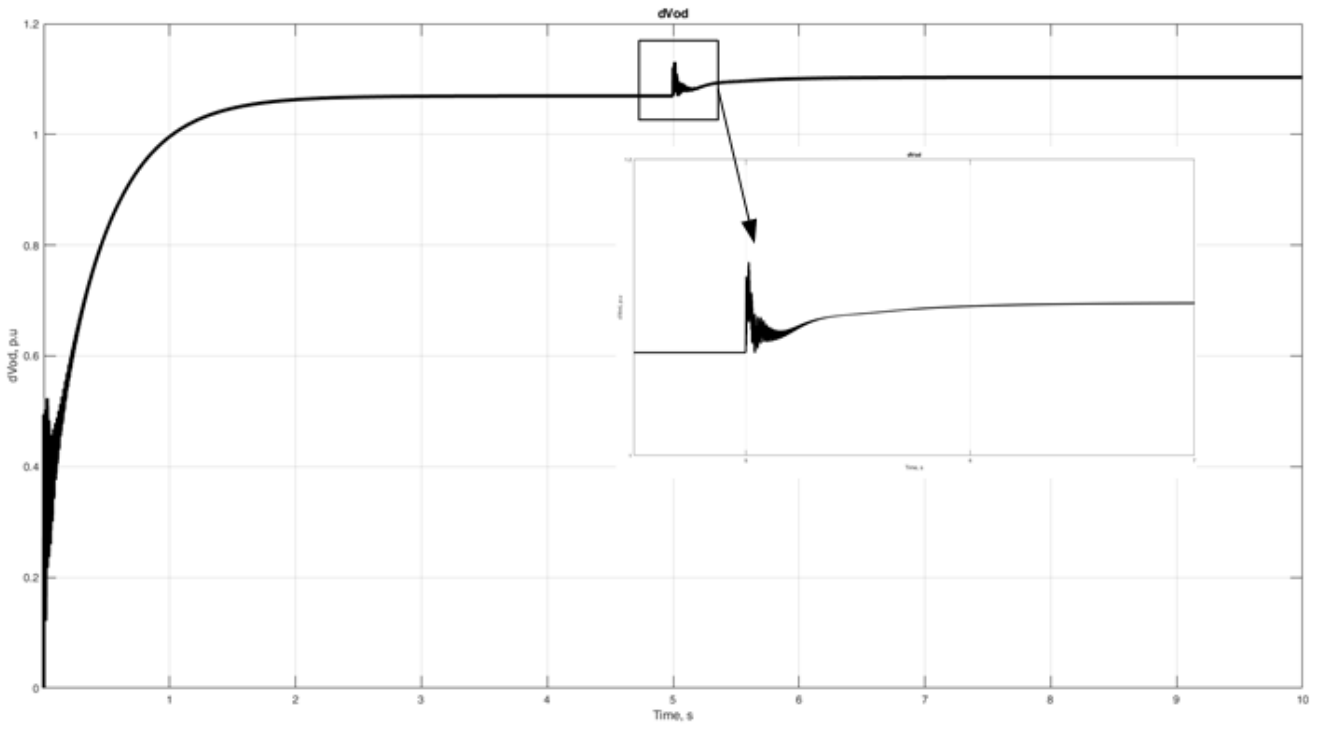


Figure 22 – Change of voltage

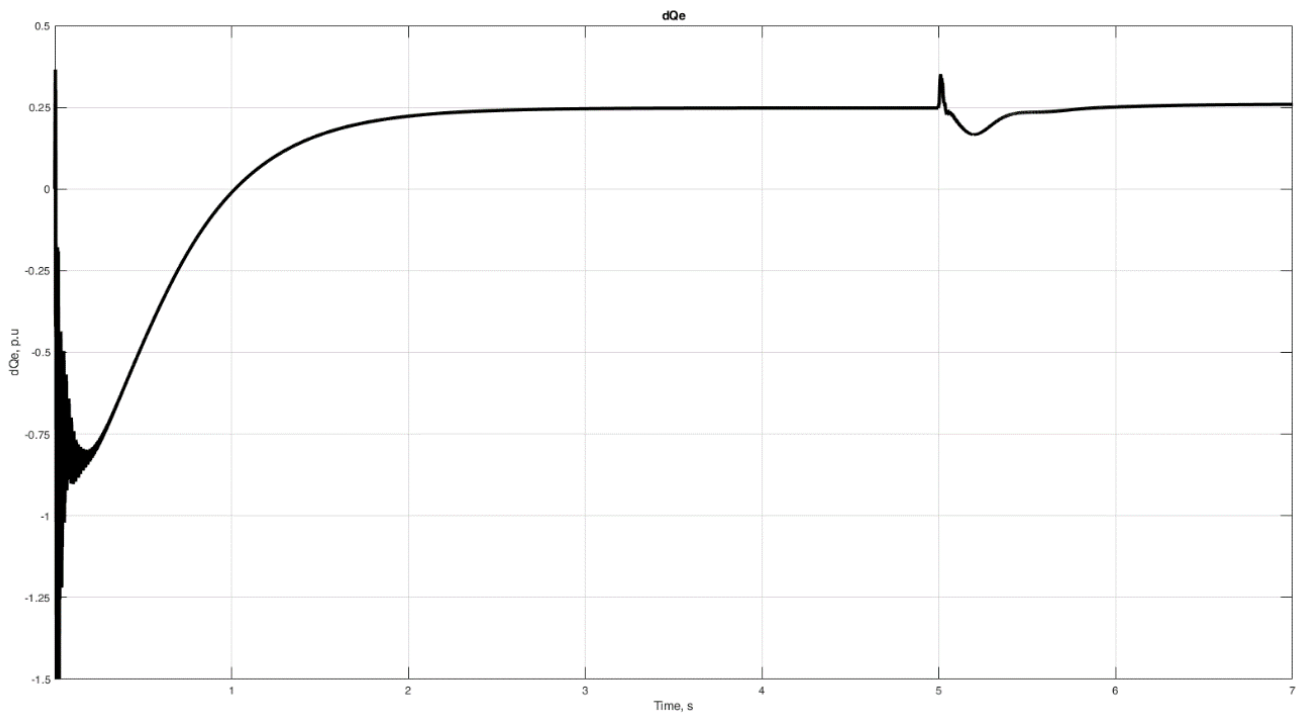


Figure 23 – Change of reactive power

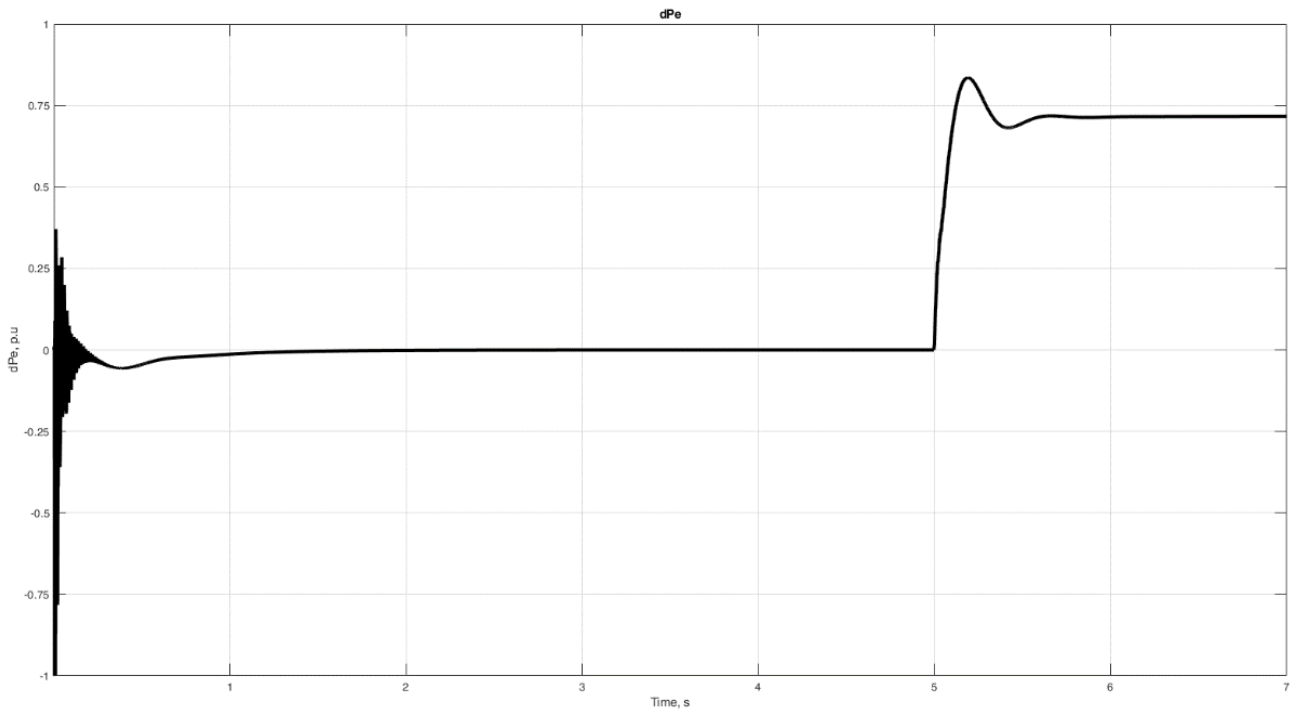


Figure 24 – Change of active power

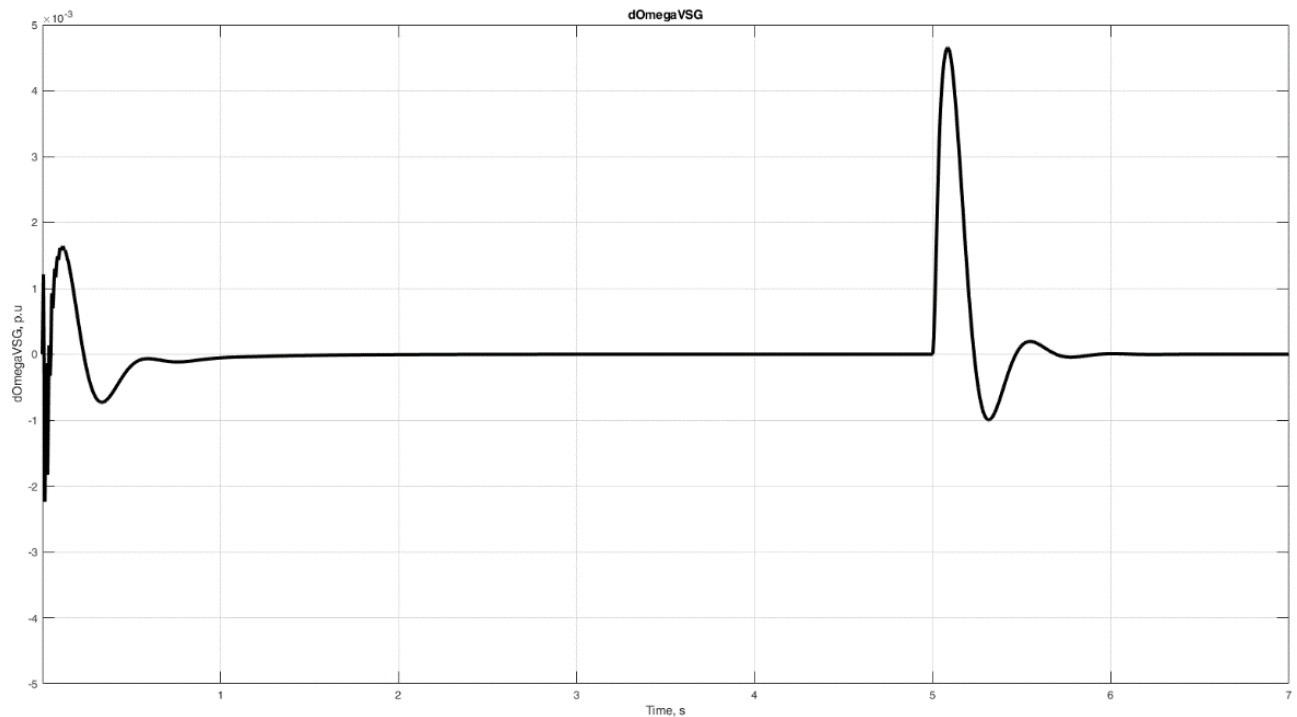


Figure 25 – Change of frequency deviation

From these curves it can be seen that regulation of VSG-C works: when the voltage and frequency deviation occur governing system return their values to the rated ones.

3.3. Investigation of detailed non-linear model

Model in PSCAD allows to investigate detail response of topology due to the fact that this model includes all parts basic modules of inverter, main electrical equipment of grid and detailed models of electrical elements.

Structurally this is a model of 2 machine system. The transient starts when frequency decreases by 0.5 Hz at 5 seconds.

Curves of voltage, active power and reactive power are represented in figures 26, 27 and 28.

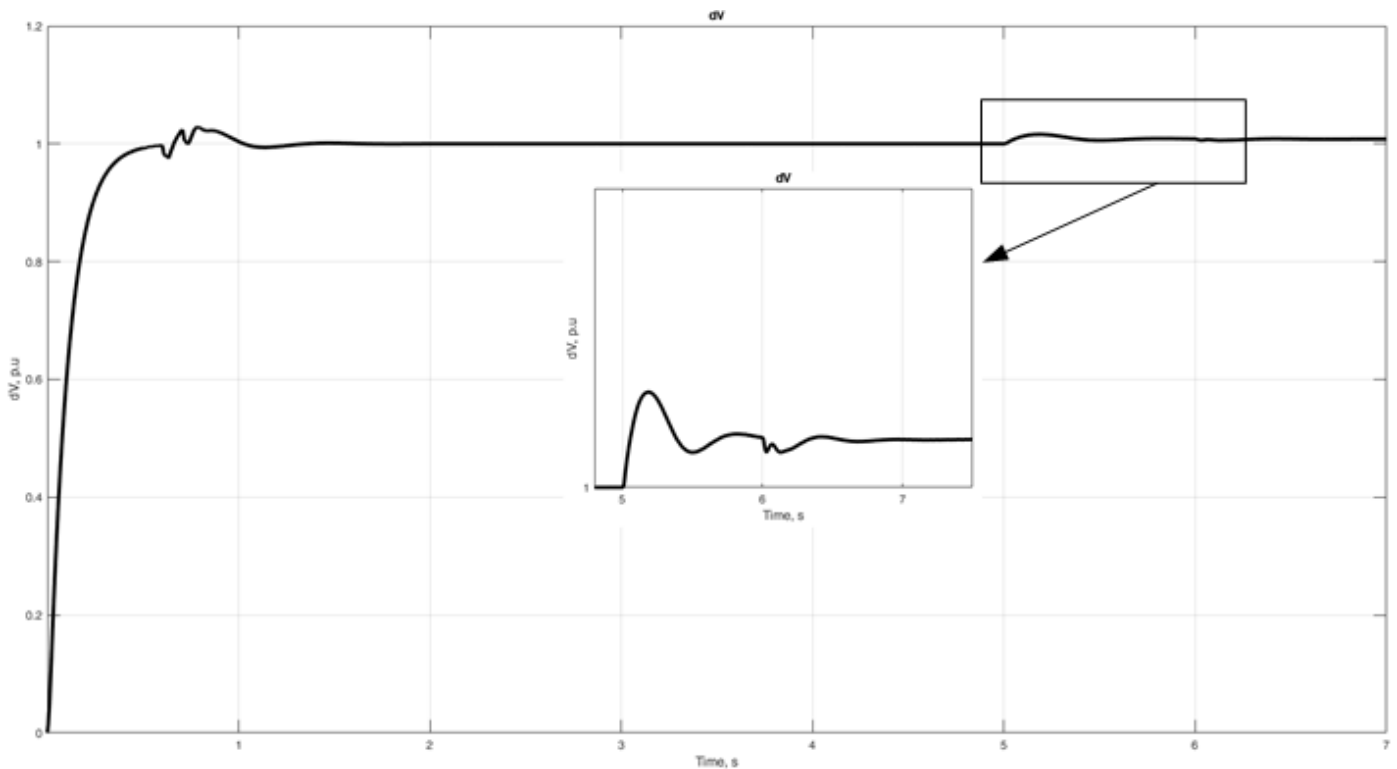


Figure 26 – Change of voltage

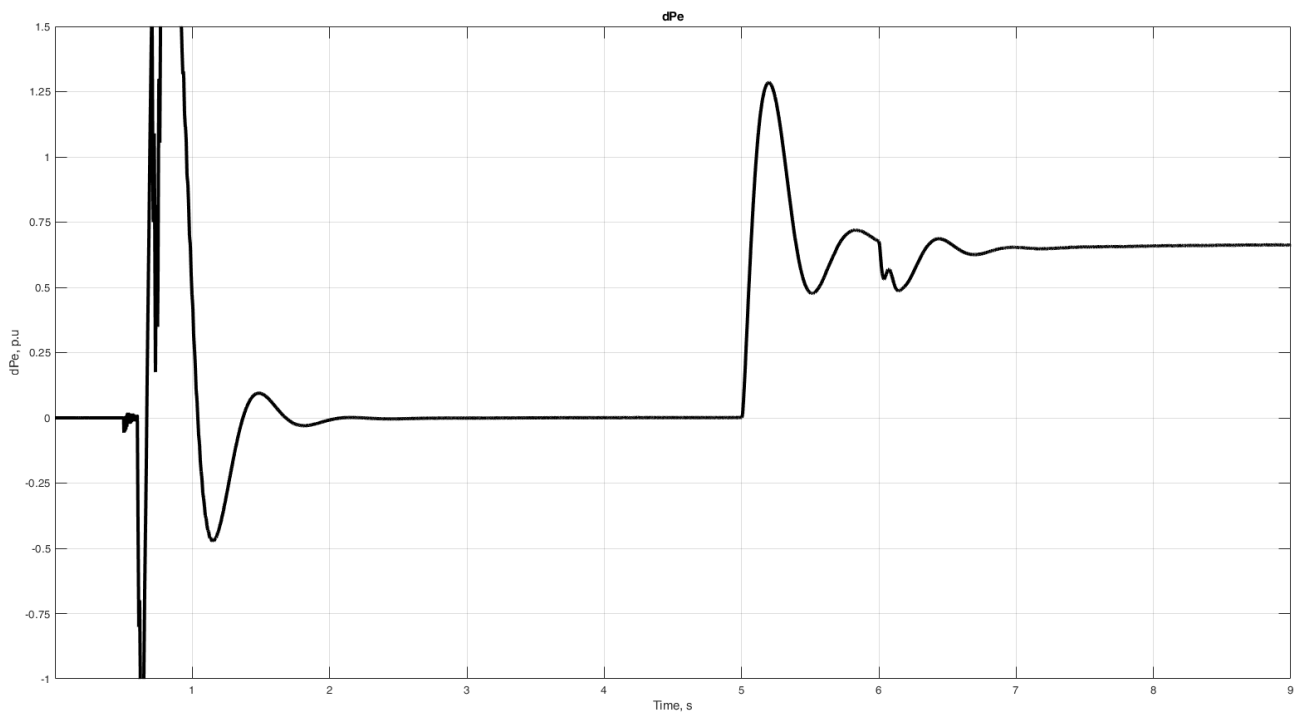


Figure 27 – Change of active power

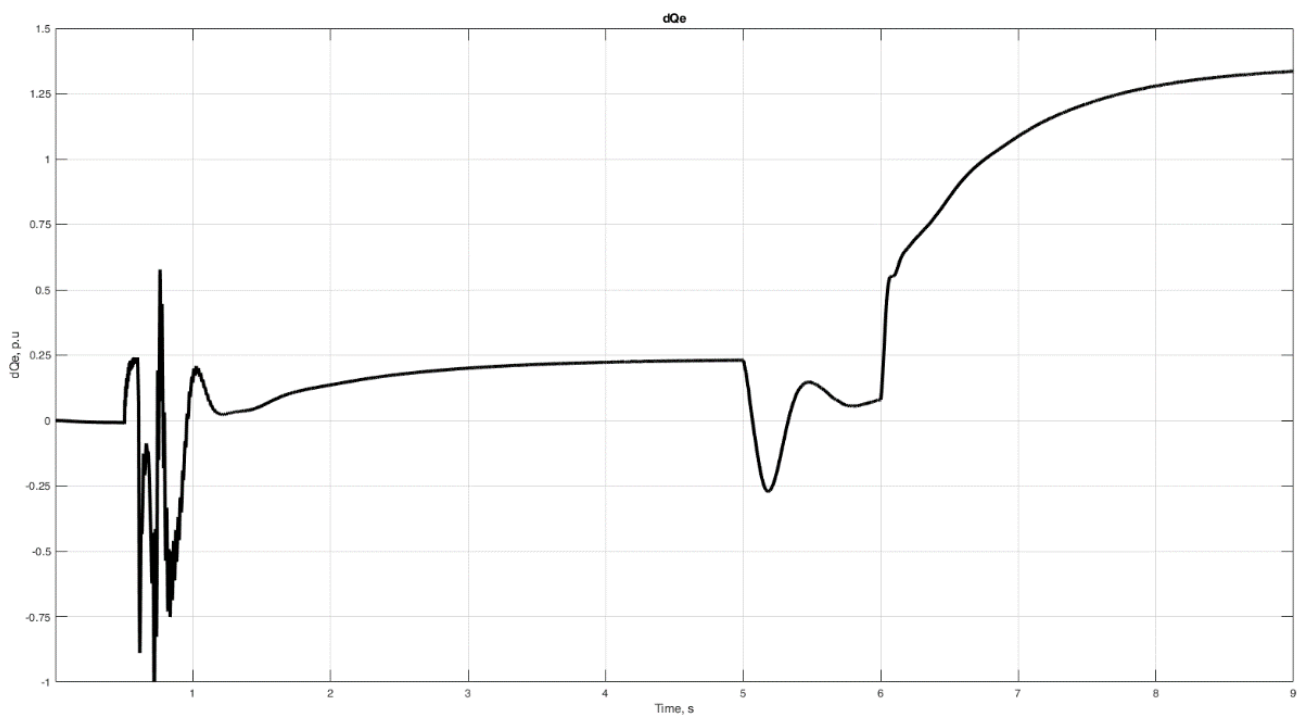


Figure 28 – Change of reactive power

Model shows familiar with linearized one response.

4. Financial management, resource efficiency and resource saving

As part of this graduate qualification work, we develop an algorithm for controlling the grid inverter of generating plants based on renewable energy sources.

The purpose of this section is to assess the impact of the grid inverter control algorithm in terms of economic efficiency and prospects, as well as resource efficiency and competitiveness of the project.

To achieve this goal in the current section it is necessary to solve the following tasks: analyze the competitive technical solutions of the project; conduct SWOT-analysis; perform planning and organization of scientific research, based on them to build a Gantt chart, as well as determine the budget and resource efficiency of the scientific project.

Potential consumers of the results of the work can be design or operating organizations.

Pre-project analysis

To analyze the consumers of the research results, it is necessary to consider the target market and conduct its segmentation.

The target market: private homes powered by off-grid electricity; power grids; industrial facilities.

Map of market segmentation for the use of the grid inverter control algorithm of generating plants based on renewable energy sources (RES).

This segmentation map shows that a grid-guided inverter control system is in demand in a broad spectrum of the market. At the moment, there is a grid slave inverter system on the market that covers the same market segments as the new development. However, this solution does not have the ability to control the amplitude and frequency of the output signal, cannot take part in the processes of voltage frequency regulation in power systems and improve its dynamic properties.

Table 4.1 – Market segmentation map for the use of the battery management system in hybrid autonomous power supply systems

	Villages, cottage communities, farms	Industrial facilities	Power grids
Network inverter control system			
Inverter network slave system			

Based on this information, we can conclude that the grid inverter control system can compete with the grid slave inverter system, as it has more functionality and can become a replacement for the obsolete development.

In this section, an analysis of the technical solution is carried out, which will allow you to determine the characteristics that describe the quality of development, as well as the prospects for its development.

The evaluation of the study is carried out according to the following groups of criteria:

1. User productivity improvement;
 - usability;
 - functional capacity (provided capabilities);
 - reliability;
 - ease of use;
 - quality of user interface.
2. Economic criteria for evaluating the effectiveness of development:
 - competitiveness of the solution;
 - the perspective of the solution;
 - implementation costs;

- financial efficiency of scientific development;
- term of implementation.

The scorecard, presented in Table 4.2, contains the technical and economic criteria for evaluating the quality of development. The evaluation card allows you to adjust the scientific research, because it provides for its certain technical and economic features of development, creation and commercialization. Comparison will be made for the grid inverter control system and the grid slave inverter system. The maximum score characterizes the complete fulfillment of one or another indicator. Technical criteria are defined according to the requirements for this development. The economic criteria are defined according to the financial possibilities, as well as the relevance and the stage of readiness of the technical solution.

Table 4.2 – Scorecard for comparing competitive technical solutions (developments)

Assessment Criteria	Criterion weight	Scores		Competitiveness	
		Fact.	Max.	Network inverter control system	GFM system
1	2	3	4	5	6
Technical criteria for assessing the quality of design					
Energy Efficiency	0.20	80	100	0.80	0.60
Ease of use	0.05	85	100	0.80	0.65
Service life	0.10	60	100	0.60	0.60
Reliability	0.15	70	100	0.80	0.80
Eco-friendliness	0.10	100	100	0.60	0.60
Economic criteria for assessing the effectiveness of development					
Costs of implementation	0.10	70	100	0.75	0.60
Maintenance	0.10	85	100	0.60	0.60
Fuel costs	0.15	95	100	0.95	0.95
Implementation period	0.05	95	100	0.75	0.60
Total	1			5.90	5.40

The analysis of competitive technical solutions is determined by the formula:

$$I_{av} = \sum W_i \cdot S_i \quad (4.1)$$

where I_{av} – the weighted average value of the indicator of quality and prospects of scientific development; B_i – indicator weight (in fractions of one); S_i – score of the i -th indicator.

Thus, as a result of the analysis of competitive technical solutions, the final value of the quality index and perspective of the Network Inverter Control System was 5.90, and the Network Slave Inverter System was 5.40, which indicates that the developed solution is the most promising.

FAST-analysis

FAST-analysis is synonymous with the functional-value analysis. The essence of this method is based on the fact that the costs associated with the creation and use of any object that performs a given function, consists of the necessary for its manufacture and operation and additional, functionally unjustified, excess costs that arise from the introduction of unnecessary functions not directly related to the purpose of the object, or associated with imperfect design, technological processes, materials used, methods of labor, etc.

Conducting a FAST analysis involves six stages:

1. Selection of the object of the FAST analysis.
2. Description of the main, main and auxiliary functions performed by the object.
3. Determination of the significance of the functions performed by the object.
4. Analysis of the cost of functions performed by the object of study.
5. Construction of the function-cost diagram of the object and its analysis.
6. Optimization of functions performed by the object.

Stage 1. Selection of the object of FAST analysis.

Within the framework of the master's thesis, the object of the FAST-analysis is a hybrid autonomous power supply system with batteries, solar panels, wind turbines, diesel generator, as well as an intelligent unit aimed at rational coordination of generated and consumed electricity.

Stage 2. Description of the main, main and auxiliary functions performed by the object.

Stage 3. Determination of the significance of the functions performed by the object.

The method of prioritization proposed by Blumberg V.A. and Gluschenko V.F. is used to assess the significance of functions. This method is based on the calculation-expert determination of the significance of each function.

At the first stage a function adjacency matrix is built, where "<" - less significant; "=" - equal functions in importance; ">" - more significant.

At the first stage a function adjacency matrix is built, where "<" - less significant; "=" - equal functions in importance; ">" - more significant.

Table 4.3 – Adjacency matrix

	Function 1	Function 2	Function 3
Function 1	=	<	<
Function 2	>	=	<
Function 3	>	>	=

The second step involves converting the adjacency matrix into a matrix of quantitative function relations: 0.5 for "<", 1.5 for ">", 1 for "=".

Table 4.4 – Matrix of quantitative relations of functions

	Function 1	Function 2	Function 3	Total
Function 1	1	0.5	0.5	3.5
Function 2	1.5	1	0.5	3
Function 3	1.5	1.5	1	2

Table 4.5 – Classification of functions performed by the object of research

Name of the detail (unit, process)	Number of details	Function in progress	Function range		
			Head	Main	Auxiliary
Managed inverter	1	Forms the type of output signal; Sends commands to enable/disable energy storage devices	X		
RES-electric installation	1	Converts primary renewable en- ergy into electrical energy		X	
Storage battery	1	Stores and outputs electrical en- ergy			X

Table 4.6 – Determination of the value of the functions performed by the object of research

Name of the detail (unit, process)	Quantity parts per unit	Function in progress	Norm consumption rate, kg	The labor intensity of the part, norm-h.	The cost, rubles.	Salary, rub./piece	Self-cost, rub.
Managed inverter	1	Forms the type of output signal. Sends commands to enable/disable energy storage devices	-	24	335 200	22900	358 100
RES-electric installation	1	Converts primary renewable energy into electrical energy	-	10	60 000	5000	65 000
Storage battery	1	Stores and outputs electrical energy	-	48	163 000	5000	168 000
Total							591 100

Calculate the relative importance of each function:

1) Controlled inverter: $3.5/8.5 = 0.41$;

2) RES-electric plant: $3/8.5 = 0.35$;

3) Battery pack: $2/8.5 = 0.24$;

Stage 4. Analysis of the value of the functions performed by the object of research.

The task of this stage is to assess the level of costs for each function with the help of special methods. The calculation of the cost of functions is shown in Table 4.6.

The total cost of production is 591 100 rub.

Let's calculate the relative cost of each function:

1) Managed inverter: $\frac{358\ 100}{591\ 100} = 0.606$;

2) RES-electric installation: $\frac{65\ 000}{591\ 100} = 0.110$;

3) Storage battery: $\frac{168\ 000}{591\ 100} = 0.284$;

Stage 5. Construction of the function and cost diagram of the object and its analysis.

Information about the object of research, collected during the previous stages, at this stage is summarized in the form of a functional-value diagram (FVD).

The functional-cost diagram in allows to reveal disproportions between the importance (usefulness) of the functions and the costs of them. Analysis of the FDS shows a clear presence of disproportion on function 2. It is necessary to work on the elimination of these disproportions.

Stage 6. Optimization of functions performed by the object.

List of measures to reduce costs per unit effect:

- Cost reduction with a reasonable reduction of technical parameters to their functionally necessary level;
- Application of fundamentally new design solutions;

- Optimization of technical parameters;
- Optimization of reliability parameters;
- Improved maintainability;
- Application of new processes, blanks, materials, etc.

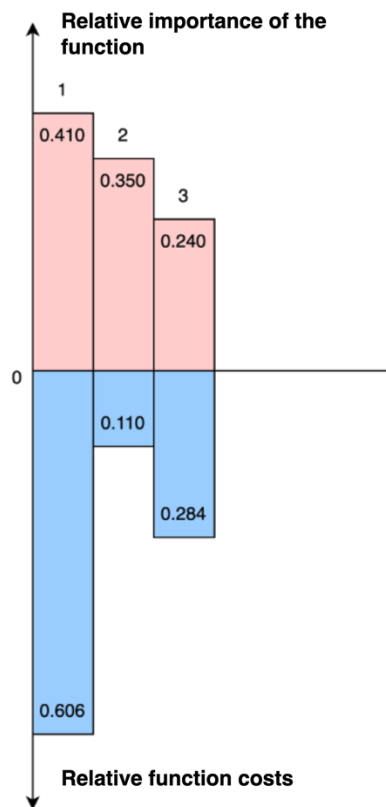


Figure 29 – Functional Cost Diagram

SWOT-analysis

The SWOT analysis is conducted to analyze the internal and external factors that can affect the research project. Its matrix allows you to determine the mutual influence of the factors and draw conclusions that will help in the development of the research strategy. The strengths and weaknesses can include the internal features of the research study, and the opportunities and threats can include the characteristics of the external environment. The analysis results in a matrix, presented in the form of Table 4.7.

Table 4.7 – SWOT analysis matrix of the research project

	<p>Strengths:</p> <p>S1. Improvement of inertia properties of power systems.</p> <p>S2. Involvement of RES-electric plants in participation in regulation of voltage frequency of power systems.</p> <p>S3. Environmental friendliness of the technology.</p>	<p>Weaknesses:</p> <p>W1. High cost of implementation.</p> <p>W2. The need for many preliminary studies.</p> <p>W3. Complex service.</p>
<p>Opportunities:</p> <p>O1. Solving the problems that slow down the growth of RES capacity implementation.</p> <p>O2. Qualitative improvement of processes in energy systems.</p> <p>O3. Public and private support for industrial modernization projects.</p>	<p>Improving the inertia properties of power systems can lead to a qualitative improvement in power system processes.</p> <p>Involvement of RES power plants in the regulation of voltage frequency of power systems can solve the problem of the slow growth of the introduction of RES capacity</p> <p>Green technology can attract public and private support for the project.</p>	<p>High cost and more complicated service makes it difficult to introduce devices everywhere; the solution to the problem can be state subsidization of projects to modernize power facilities.</p> <p>A large number of tests will reduce the risks of malfunctions.</p>
<p>Threats:</p> <p>T1. Lack of demand for technology.</p> <p>T2. Emergence of emergencies due to errors in the algorithm.</p>	<p>The threats to the project are related to temporary difficulties. Lack of demand is prevented by continuous improvement of the grid inverter control algorithm. Competent staff support will reduce the possibility of malfunction.</p>	<p>To implement this project requires financial and labor costs of staff, which is a deterrent to the implementation of the development.</p>

The following conclusions can be drawn from the SWOT analysis: The study has a significant number of strengths. The grid inverter control system is able to improve the inertia properties of power systems, as well as reduce the negative impact on the environment. There are also some disadvantages, which can be solved with labor and financial resources.

Project initiation

A group of initiation processes consists of processes that are performed to define a new project or a new phase of an existing project. The initiation processes define the initial goals and content and capture the initial financial resources. The internal and external stakeholders of the project that will interact with and influence the overall outcome of the research project are identified. This information is captured in the Project Charter.

The Project Charter documents the business needs, the current understanding of the needs of the project customer, and the new product, service, or outcome to be created.

This section provides information about the project stakeholders, the hierarchy of project goals, and the criteria for achieving the goals. This information is presented in Tables 4.8 and 4.9.

Table 4.8 – Project stakeholders

Project stakeholders	Stakeholder expectations
Power grid companies, enterprises and private consumers	Improving the reliability and stability of power systems and power quality,
Companies manufacturing and selling batteries, power electronics and inverters	Expansion of the range of goods offered, increase in demand
Project developer	Self-fulfillment in the electric power industry

Table 4.9 – Project goals and results

Project goals:	Development of a power inverter control algorithm to simulate the behavior of a synchronous machine in the area of inertial properties and frequency control.
Expected project results:	Improving the inertia properties of power systems, improving their dynamic properties through the participation of renewable energy facilities in frequency regulation.
Acceptance criteria for the result of the project:	The workability of development, safety, cost-effectiveness, environmental friendliness
Requirements for the result of the project:	Requirements:
	Workability
	Safety
	Economy
	Eco-friendliness

At this stage of the work the following questions are solved: who will be in the working group of this project, the roles of each of the participants and their labor costs in the project are determined. This information is shown in Table 4.10.

Table 4.10 – Project working group

№	Full name, main place of work, position	Role in the project	Functions	Labor costs, hours.
1	A.A. Suvorov, TPU, Associate Professor	Project expert	Responsible for the implementation of the project within the specified resource limits, coordinates the activities of the project participants.	104

Table 4.10 (continued)

2	L.Y. Spitsyna, TPU, Associate Professor	Project financial management expert	Responsible for supervising the Financial Management section of the project	40
3	O.A. Antonevich. TPU, Associate Professor	Project expert on social responsibility	Responsible for supervising the "Social Responsibility" section of the project	16
4	B.D. Mal'yuta, TPU, student	Project performer	Specialist, who performs some works under the project	928
Total:				1088

Project constraints are all factors that may serve to limit the degree of freedom of the project team members, as well as "project boundaries" - the parameters of the project or its product, which will not be implemented as part of this project.

Table 4.11 – Limitations of the project

Factor	Limitations/assumptions
Project budget	Not more than 500 000 rubles.
Financing source	TPU
Project timeline	1.09.2022-1.06.2023
Date project management plan is approved	10.01.2022
Project completion date	30.05.2023
Other restrictions and assumptions	-

Science and technology management planning

A group of planning processes consists of processes performed to determine the overall content of work, clarify goals, and develop a sequence of activities required to achieve these goals.

When organizing a project, it is necessary to optimally plan the timing of the work. Table 4.12 identifies the key events of the project, their dates and results.

Table 4.12 – Project control events

№	Controlling event	Date	Result (confirming document)
1	Development of the terms of reference	10.01.2023	Job form
2	Choice of design direction	17.01.2023	Report
3	Development of the schedule	31.01.2023	Timetable
4	Theoretical research	10.02.2023	Report
5	Solution development	15.03.2023	Graphs, calculations
6	Process modeling	21.04.2023	Research report
7	Formalization of the explanatory note	30.05.2023	Explanatory note

At this stage, a complete list of work to be carried out, their performers are determined and the optimal duration.

The result of work planning is a calendar plan, presented in Table 4.13, where the executors: S - supervisor, PE - Project Executor (student), E by FM - project expert on financial management, and E by SR - project expert on social responsibility.

Table 4.13 – Project calendar

№	Title	Duration, days	Starting date	Completion date	Performers
1	Drawing up and approval of the terms of reference	4	09.01.2023	12.01.2023	S
2	Selection and study of materials on the topic	11	13.01.2023	24.01.2023	PE
3	Development of the schedule	4	25.01.2023	29.02.2023	S
4	Description of the topic relevance	2	31.01.2023	02.02.2023	PE
5	Research of existing implementations	2	03.02.2023	05.02.2023	PE
6	Mathematical modeling of the selected algorithm	7	06.02.2023	13.02.2023	PE
7	Linearization of the model and study of it in the state space and through modal analysis in the Matlab Simulink software package	19	14.02.2023	03.03.2023	PE
8	Transfer of the model into the PSCAD software package	15	04.03.2023	18.03.2023	PE
9	Investigation of the model within the framework of the two-machine system problem	10	19.03.2023	29.03.2023	PE

Table 4.14 (continued)

10	Porting of this model to the RTDS software-hardware system	20	30.03.2023	19.04.2023	PE
11	Research of the model as a part of the real part of the Irkutsk power system	3	20.04.2023	22.04.2023	PE
12	Evaluation of research results	5	29.04.2023	03.05.2023	S
13	Evaluation of the economic efficiency of the investigated technology оуисследуемой технологии	13	04.05.2023	17.05.2023	PE, E by FM
14	Consideration of social responsibility issues	5	18.05.2023	23.05.2023	PE, E by SR
15	Drafting an explanatory note	16	17.05.2023	28.05.2023	PE

The Gantt chart allows you to graphically display the sequence and timing of each stage of the SRC, it is a calendar schedule of works with a breakdown by months and decades.

According to the diagram, the duration of work in calendar days of the project manager is 13 days, the executor of the project (student) 116 days, the project expert on financial management 5 days, and the project expert on social responsibility 2 days.

In order to determine the budget for the project, the following cost items must be considered:

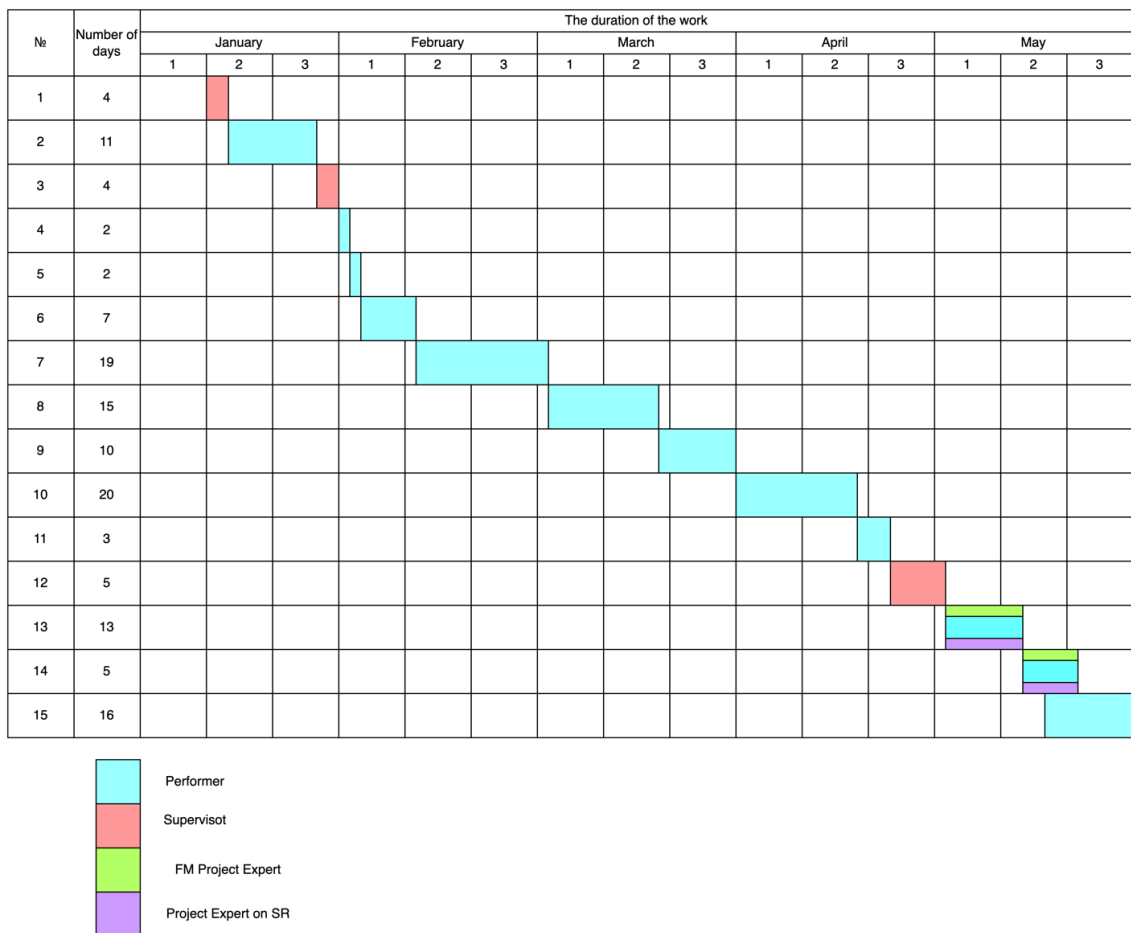


Figure 30 – Gantt chart

- 1) Research software;
- 2) Material resources;
- 3) Working group salaries;
- 4) Additional salaries of the working group;
- 5) Contributions to non-budgetary funds;
- 6) Overhead costs.

The item basic salary includes the salaries of the employees directly involved in the study: the head and the engineer. Salary costs are determined depending on the labor intensity of the work performed, calculated earlier, as well as the current system of salaries and tariff rates, for each performer. Also included in the basic salary is a bonus, which must be paid each month from the wage fund in the amount of 20-30% of the tariff or salary.

The item includes the basic salary of employees directly engaged in the implementation of STI, (including bonuses, additional payments), as well as additional wages:

$$C_{3\Pi} = 3_{\text{OCH}} + 3_{\text{доп}} \quad (4.2)$$

where 3_{OCH} – basic salary, $3_{\text{доп}}$ – extra pay (12-20 % от 3_{OCH}).

The basic salary (3_{OCH}) is calculated by the following formula (as an example of calculating the salary of a project performer (student):

$$3_{\text{OCH}} = 3_{\text{дн}} \cdot T_{\text{раб}} = 973,898 \cdot 109 = 106154.915 \text{ rub}$$

where $T_{\text{раб}}$ – duration of work performed by the scientific-technical worker, working days; $3_{\text{дн}}$ – average daily wage of an employee, rubles.

The average daily wage is calculated by the formula, rubles:

$$3_{\text{дн}} = \frac{3_{\text{м}} \cdot \text{M}}{F_{\text{д}}} = \frac{22100 \cdot 10,4}{236} = 973.898 \text{ rub.} \quad (4.3)$$

where $3_{\text{м}}$ – employee's monthly salary, rubles; M – number of months of work without leave during the year: with 48 working days leave - M = 10.4 months, 6-day week; $F_{\text{д}}$ – actual annual fund of working time of scientific and technical personnel, working days. (Table 4.14).

$$3_{\text{м}} = 3_{\text{б}} \cdot (k_{\text{нп}} + k_{\text{д}}) \cdot k_{\text{р}} = 3_{\text{б}} \cdot k_{\text{р}} = 17000 \cdot 1.3 = 22100 \text{ rub.} \quad (4.4)$$

where $3_{\text{б}}$ – base salary, rubles.; $k_{\text{нп}}$ – bonus factor; $k_{\text{д}}$ – coefficient of surcharges and bonuses; $k_{\text{р}}$ – regional coefficient of 1.3 (for Tomsk).

Table 4.14 – Balance of working time

Working time indicators	Project expert	Project Performer (student)	Project expert on FM	Project expert on SO
Calendar number of days	365	365	365	365
Number of non-working days: - weekends and holidays	67	67	67	67
Loss of work time: - Vacation and sick leave	62	62	62	62
Actual annual working time fund	236	236	236	236

The calculation of basic wages is shown in Table 4.15.

Table 4.15 – Calculation of the basic salary

Executors	$З_б$, rub.	k_p	$З_м$, rub.	$З_{дн}$, rub.	$T_{раб}$, working days	$З_{оч}$, rub.
Supervisor	36800	1.3	47840	3149	13	58173
Project financial management expert	21760	1.3	28288	1862	116	192977
Project expert on social responsibility	36800	1.3	47840	3149	5	15745
Project performer	36800	1.3	47840	3149	2	6298
Total:						273192

This item includes the amount of payments stipulated by labor legislation, such as: vacation pay, seniority pay, deviations from normal working conditions, etc.

Additional wages are calculated according to the formula:

$$З_{доп} = З_{оч} \cdot k_{доп} \quad (4.5)$$

where $k_{доп}$ – coefficient of additional wages (at the design stage it is taken equal to 0.10÷0.15).

For the project manager: $З_{доп} = З_{оч} \cdot k_{доп} = 58173 \cdot 0.15 = 8726$ rub.

For the project executor (student): $З_{доп} = 192977 \cdot 0.15 = 28947$ rub.

For the FM project expert: $З_{доп} = 15745 \cdot 0.15 = 2362$ rub.

For the SR project expert: $З_{доп} = 6298 \cdot 0.15 = 945$ rub.

Table 4.16 shows a form for calculating basic and additional wages.

Table 4.16 – Salaries of STI performers

Salaries	Supervisor	Project Performer (student)	Project expert on FM	Project expert on SO
Basic salary, rubles.	58173	192977	15745	6298
Additional salary, rubles.	8726	28947	2362	945
Total salary, rubles.	66899	221924	18107	7243
Total for the item C_{3II} , rub.	314173			

The item includes deductions to non-budgetary funds. The amount of deductions to non-budgetary funds is determined based on the following formula:

$$C_{\text{BHE6}} = k_{\text{BHE6}} \cdot (3_{\text{OCH}} + 3_{\text{ДОП}}) \quad (4.6)$$

where k_{BHE6} – coefficient of deductions to non-budgetary funds (pension fund, compulsory health insurance fund, social insurance fund).

Contributions to non-budgetary funds are presented in Table 4.17.

Table 4.17 – Contributions to non-budgetary funds

Executors	Basic salary, rubles.	Additional salary, rubles.
Supervisor	58173	8726
Project performer	192977	28947
Project financial management expert	15745	2362
Project expert on social responsibility	6298	945
Coefficient of deductions to non-budgetary funds	0.3	
Contributions to non-budgetary funds		
Supervisor	20070	
Project performer	66577	

Table 4.17 (Continued)

Project financial management expert	5432
Project expert on social responsibility	2173
Total for the item $C_{\text{внecб}}$	94252

The cost of material costs for other expenses is calculated according to current price lists or contractual prices. The same item includes the cost of registration of documentation. The results of this item are presented in Table 4.18.

Table 4.18 – Raw materials, materials, components and purchased materials

Product name	Unit of measure	Quantity	Price per unit, rub.	Costs of materials, ($З_M$), rub.
Stationery	pcs.	1	650	650
Printing paper	unit.	1	282	282
96 sheet notebook	pcs.	1	80	80
Summary C_{np} :				1012

Costs of the organization: printing and copies of research materials, payment for electricity, payments for communication and Internet services, etc., - not included in the previous items of expenditure, are overhead costs. Their size is determined by the following formula ($k_{\text{нр}}$ – coefficient that takes into account overhead costs, adopted 15%):

$$C_{\text{накл}} = k_{\text{накл}}(З_{\text{осн}} + З_{\text{доп}}) \quad (4.7)$$

For the supervisor:

$$C_{\text{накл.руководителя}} = k_{\text{накл}}(З_{\text{осн}} + З_{\text{доп}}) = 0.15(66899) = 10034.9 \text{ rub}$$

For the project performer (student):

$$C_{\text{накл.исполнителя}} = k_{\text{накл}}(З_{\text{осн}} + З_{\text{доп}}) = 0.15(221924) = 33288.6 \text{ rub}$$

For the FM project expert:

$$C_{\text{накл.экс. по ФМ}} = k_{\text{накл}}(З_{\text{осн}} + З_{\text{доп}}) = 0.15(18107) = 2716 \text{ rub}$$

For the SR project expert:

$$C_{\text{накл.экс. по СО}} = k_{\text{накл}}(З_{\text{осн}} + З_{\text{доп}}) = 0.15(7243) = 1086.5 \text{ rub}$$

Summary:

$$C_{\text{накл}} = C_{\text{накл.руководителя}} + C_{\text{накл.исполнителя}} + C_{\text{накл.экс. по ФМ}} + C_{\text{накл.экс. по СО}} \\ = 10034.9 + 33288.6 + 2716 + 1086.5 = 47126 \text{ rub}$$

This section includes costs associated with the purchase of special equipment, which is necessary for work on this topic, namely devices, devices and mechanisms, control and measuring equipment, etc. The cost of special equipment in some cases is taken at the contractual price or at current price lists. The costs calculated in this section are recorded in Table 4.18.

Since this equipment is used for a long time, it is necessary to consider the cost of depreciation for this equipment:

$$A_i = \frac{S \cdot N}{H \cdot 365} \quad (4.8)$$

where A_i – amortization charge; S – hardware and software costs. N – number of days of use in the design. H – the expected service life of the equipment and software.

Calculation of depreciation rates, the results are presented in Table 4.19:

Table 4.19 – Amortization of equipment and software systems

№	Name of equipment	Quantity of equipment, units.	Cost per unit of equipment, rubles.	Amortization, rub.
1	Personal computer	1	56000	4347
2	Software license Microsoft Office	1	3400	264
Total				4611

Thus, based on the data presented in Table 4.19, the depreciation deductions for equipment and software systems amounted to 4067.6 rubles.

Based on the obtained data on individual cost items, a calculation of the planned cost of STI is made. The full cost estimate is given in Table 4.20.

Table 4.20 – Full cost estimates

Name of the article	Costs, rubles.
1. Basic salaries	273192
2. Contributions to non-budgetary funds	94252
3. Other costs	1012
4. Overhead costs	47126
5. Amortization	4611
Project budget	420193

Thus, in this section, a technical and economic study was carried out:

- the structure of the work and on its basis the calculations of the research work complexity and its budget were made;
- the budget of research work costs was calculated, which amounted to 420193 rubles.

The assessment of the comparative effectiveness of the study is based on determining the integral index of resource efficiency, which has the following form:

$$I_{pi} = \sum a_i \cdot b_i \quad (4.9)$$

where I_{pi} – integral resource efficiency indicator; a_i – importance coefficient of the i -th parameter; b_i – is the ball rating of the i -th parameter, which is set by the expert method on the selected evaluation scale.

The calculation of the integral resource efficiency indicator is presented in Table 4.21.

Table 4.21 – Comparative evaluation of project characteristics

Criteria	Importance factor	Development score
1. Safety	0,25	5
2. Reliability	0,15	4
3. Usability	0,20	3
4. Estimated service life	0,15	4
5. Energy efficiency	0,25	5
Total	1,00	

Integral resource efficiency indicator for the research project under development:

$$I_{pi} = 0.25 \cdot 5 + 0.25 \cdot 5 + 0.20 \cdot 4 + 0.15 \cdot 4 + 0.15 \cdot 3 = 4.35;$$

Thus, the integral index of resource efficiency was 4.35 out of a possible 5, indicating the effectiveness of the technical project.